

QC
807.5
.U6
A7
no.141

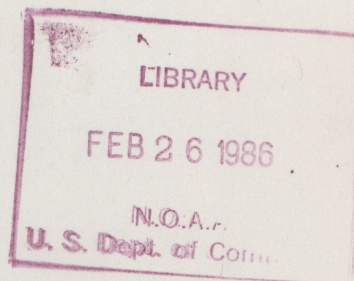
A Technical Memorandum ERL ARL-141



ON THE USE OF MONITORED AIR CONCENTRATIONS
TO INFER DRY DEPOSITION (1985)

B. B. Hicks
D. D. Baldocchi
R. P. Hosker, Jr.
B. A. Hutchison
D. R. Matt
R. T. McMillen
L. C. Satterfield

Air Resources Laboratory
Silver Spring, Maryland
November 1985



noaa

NATIONAL OCEANIC AND
ATMOSPHERIC ADMINISTRATION

Environmental Research
Laboratories

QC
807.5
.4647
no.141

NOAA Technical Memorandum ERL ARL-141

/ ON THE USE OF MONITORED AIR CONCENTRATIONS
// TO INFER DRY DEPOSITION (1985)

B. B. Hicks
D. D. Baldocchi
R. P. Hosker, Jr.
B. A. Hutchison
D. R. Matt
R. T. McMillen
L. C. Satterfield

Air Resources Laboratory
Silver Spring, Maryland
November 1985



**UNITED STATES
DEPARTMENT OF COMMERCE**

**Malcolm Baldrige,
Secretary**

**NATIONAL OCEANIC AND
ATMOSPHERIC ADMINISTRATION**

**Anthony J. Calio,
Administrator**

**Environmental Research
Laboratories**

**Vernon E. Derr,
Director**

NOTICE

Mention of a commercial company or product does not constitute an endorsement by NOAA Environmental Research Laboratories. Use for publicity or advertising purposes of information from this publication concerning proprietary products or the tests of such products, is not authorized.

CONTENTS

	Page
ABSTRACT	1
1. INTRODUCTION.....	1
2. LIMITATIONS AND CONSTRAINTS	2
3. REQUIREMENTS FOR RESOLUTION AND ACCURACY	4
4. EFFECTS OF DIURNAL VARIABILITY	5
5. EVALUATION OF v_d FROM ROUTINE DATA	11
5.1 Mathematical Derivation	15
5.2 Evaluating Aerodynamic Resistance, r_a	18
5.3 Quasi-laminar Layer Resistance, r_b	19
5.4 Surface, or Canopy Resistances, r_c	21
5.5 Canopy Wetness	23
5.6 Effects of Canopy Phenology	26
6. INTERPRETIVE MODEL	27
7. CONCLUSIONS	29
ACKNOWLEDGEMENTS	30
REFERENCES.....	31
Appendix A: Some Special Considerations	35
Integrations of Detailed Information	35
Adaptive Ecological Characteristics of Plant Communities	36
Snow and Liquid Water Surfaces	37

Urban Areas	37
Appendix B: Modeling Trace Gas Exchange in Canopies	38
Introduction	38
Stomatal Resistances, r_s	38
Mesophyll Resistances, r_m	41
Combining Stomatal and Mesophyll Resistances	42
Cuticular Resistance	42
Extension to Entire Canopy	42
Appendix C: Particle Deposition to Canopies	48
Background	48
Estimating Particle Deposition	48
Appendix D: Program Listing and Explanation	53
Discussion	53
Listing	60

FIGURES

- Figure 1.--Hypothetical diurnal cycles of air concentration of a chemical species and the corresponding deposition velocity, selected to demonstrate how the product of long-term averages can differ from the average product. 6
- Figure 2.--Average diurnal cycles of near-surface concentrations of sulfate ammonium, and nitrate aerosol, as reported by Johnson et al. (1981) for rural sites located at Raquette Lake, NY (A); Brookhaven National Laboratory, Upton, Long island, NY (B); Rockport, IN (C); Charlottesville, VA (D); and State College, PA (E). Concentrations are all in micrograms per cubic meter. 8
- Figure 3.--Ozone concentrations recorded at the Tennessee site of the dry deposition "core" monitoring program, as identified in Figure 5. 9
- Figure 4.--Examples of sulfur dioxide records obtained concurrently with the O₃ data of Figure 3 at the Tennessee dry deposition "core" monitoring site, as shown in Figure 5. Note the evidence of fumigation episodes on the last day. 10
- Figure 5.--Sites selected for tests of dry deposition monitoring techniques, with emphasis on the three "core" stations presently in operation (as of June, 1984) at Argonne, Illinois; State College, Pennsylvania, and Oak Ridge, Tennessee. 12
- Figure 6.--The variation with time of the deposition velocity for HNO₃, computed using the methods described in the text during a test of an on-line microprocessor to analyze data from meteorological sensors. Calculations were performed as if the exposure were appropriate for a forest. 13
- Figure 7.--The resistance model which forms the basis for data evaluation, showing the three major resistance components (r_a , r_b and r_c) in series and showing the way in which individual resistances to transfer to different receptor surfaces combine into an effective canopy as residual resistance, r_c . In every case, major variables affecting individual resistances are identified. As an example of the way different pollutants follow different paths, the dotted line illustrates the probable route associated with SO₂ transfer. In contrast, a highly reactive trace gas like HF or HNO₃ would be expected to deposit quickly via almost all available routes. 14

	Page
Figure 8.--The variation with surface roughness Reynolds number of the boundary-layer resistance indicator, ku_*r_b (see text), as determined for the case of heat transfer. Shaded areas represent field data (as summarized by Garratt and Hicks, 1973) with the upper branch being associated with bluff roughness elements and the lower branch representing vegetation and fibrous roughness elements. The dashed and dotted curves represent formulae derived by Owen and Thompson (1963) and Brutsaert (1975), respectively.	17
Figure 9.--A schematic illustration of the pathways and processes for transfer between air and plant tissue (following O'Dell et al., 1977).	21
Figure 10.--The probability of surface wetness (due to all causes, including dewfall and precipitation) at the forest meteorology research site adjacent to the Walker Branch Watershed, Oak Ridge, Tennessee, over the period from July 1981 to June 1984.	24
Figure 11.--Residual resistances (i.e., estimated values of r_c) for ozone and water vapor transfer, computed from eddy flux data obtained over a maize canopy (after Wesely et al., 1978). B.1. Vertical distribution of leaf area index for a fully-leaved deciduous forest in summer. The data were obtained at the oak-hickory forest meteorology research site in Oak Ridge, Tennessee.	27
Figure B.1.--Vertical distribution of leaf area index for a fully-leaved deciduous forest in summer. The data were obtained at the oak-hickory forest meteorology research site in Oak Ridge, Tennessee.	43
Figure B.2.--Bulk canopy stomatal resistance to water vapor exchange (\bullet), carbon dioxide (Δ), ozone (\blacktriangle), and sulfur dioxide (\circ), computed to demonstrate the dependence on photosynthetically active radiation using a multi-layer model of a soybean canopy (Baldocchi et al., 1985).	45
Figure B.3.--Bulk canopy stomatal resistance to sulfur dioxide transfer for four different canopies, oak (\bullet), spruce (Δ), maize (\blacktriangle), and soybeans (\circ), derived using the same model as in Figure B.2.	46
Figure B.4.--The effects of leaf area index on canopy stomatal resistance computed as in Figure B.2, for LAI = 1(Δ), 3(\blacktriangle), and 5(\circ). Values derived using the simple methods of Table 2 are also shown as dotted lines.	47

	Page
Figure C.1.-The conceptual resistance model associated with the transfer of particles. The term $r_a \cdot r_s \cdot v_g$ is included to satisfy the formalism of Equation C.7.	50
Figure C.2.-Fine-particle deposition velocity as a function of $\sigma_0 \cdot u$, with standard error and the number of contributing measurements indicated. Values were obtained over a deciduous forest in winter, with no snow present (see Wesely et al., 1983).	52
Figure D.1.-The weekly-average diurnal cycle of deposition velocity for HNO_3 , SO_2 , O_3 , and NO_2 , deduced for the Oak Ridge site using the methods described here, for the first week of 1985.	54
Figure D.2.-The weekly-average diurnal cycle of deposition velocity for HNO_3 , SO_2 , O_3 , and NO_2 , deduced for the Oak Ridge site using the methods described here, for the second week of 1985.	55
Figure D.3.-The weekly-average diurnal cycle of deposition velocity for HNO_3 , SO_2 , O_3 , and NO_2 , deduced for the Oak Ridge site using the methods described here, for the third week of 1985.	56
Figure D.4.-The weekly-average diurnal cycle of deposition velocity for HNO_3 , SO_2 , O_3 , and NO_2 , deduced for the Oak Ridge site using the methods described here, for the fourth week of 1985.	57
Figure D.5.-Weekly-averaged diurnal cycles of deposition velocity for HNO_3 , as deduced from the routines described here, for locations near Oak Ridge (TN), West Point (NY), State College (PA), and Whiteface Mountain (NY). Data are for the first week of 1985.	59
Table 1.--Shows molecular and Brownian diffusivities for a range of pollutants and deduced values of Schmidt numbers.	22
Table 2.--Summary of relations contributing to first-order evaluation of canopy resistance for particles and trace gases.	25
Table B.1.--Shows results of experimental studies of the relationship between stomatal resistance and photosynthetic radiation intensity.	40
Table B-2.--Shows characteristic temperatures associated with the stomatal resistance of different species.	45

SYMBOLS

$a(T)$	Temperature coefficient controlling r_c	
A	Site-specific "neutral" value of σ_θ	
b	Coefficient controlling stomatal conductance	$[m^2/W]$
b_e	Coefficient in expression for f_e	$[1/mb]$
b_T	Coefficient in expression for f_T	
b_w	Coefficient in expression for f_w	
C	Atmospheric concentration	$[kg/m^3]$
C_0	Concentration at height z_{0c}	$[kg/m^3]$
d	Displacement height	$[m]$
D	Molecular or Brownian diffusivity	$[m^2/s]$
e	Vapor pressure	$[mb]$
$e_s(T)$	Saturation vapor pressure at temperature T	$[mb]$
f_e	Correction function to r'_s for humidity	
f_T	Correction function to r'_s for temperature	
f_w	Correction function to r'_s for water stress	
F_0	Estimated deposition flux	$[kg/m^2/s]$
F_p	Particle flux	$[kg/m^2/s]$
F_1	Deposition flux -- integral form	$[kg/m^2/s]$
F_2	Deposition flux -- summation form	$[kg/m^2/s]$
g	Conductance	$[m/s]$
g_s	Stomatal conductance	$[m/s]$
H	Henry's Law constant	
I	Insolation	$[W/m^2]$
I_p	Photosynthetically active radiation	$[W/m^2]$
k	von Karman constant	
L	Monin-Obukhov length scale	$[m]$

LAI	Leaf area index	
n	Integral constant	
Pr	Prandtl number ($\equiv \nu/\kappa$)	
r_{xy}	Correlation coefficient between x and y	
r_a	Aerodynamic resistance	[s/m]
r_b	Diffusive boundary layer resistance	[s/m]
r_c	Canopy or residual resistance	[s/m]
r_{cg}	Canopy resistance: gases	[s/m]
r_{cp}	Canopy resistance: particles	[s/m]
r_{cut}	Gross canopy cuticular resistance	[s/m]
r_d	Soil resistance	[s/m]
r_s	Gross canopy stomatal resistance	[s/m]
r'_c	Canopy resistance, unit area	[s/m]
r'_{cut}	Cuticular resistance	[s/m]
r'_m	Mesophyll resistance	[s/m]
r'_s	Stomatal resistance	[s/m]
r'_{sm}	Minimum stomatal resistance	[s/m]
r'_{so}	Overall resistance via stomata	[s/m]
R	Total resistance to transfer	[s/m]
Ri	Richardson number	
R_{xy}	Correlation coefficient between x and y	
RH	Relative humidity	
Sc	Schmidt number ($\equiv \nu/D$)	
t,T	Time, time interval	[s]
T	Temperature	[C]
$T_{o,l,h}$	Temperatures limiting r'_s	[C]
u	Wind speed	[m/s]

u_*	Friction velocity	[m/s]
v	Lateral wind velocity	[m/s]
v_d	Deposition velocity	[m/s]
v_g	Settling speed (particles)	[m/s]
v_p	Effective particle deposition velocity	[m/s]
w	Vertical velocity	[m/s]
W_n	Wetness of surface	
z	Height above the zero plane displacement	[m]
z_0	Roughness length, momentum	[m]
z_{0c}	Roughness length, pollutant	[m]
Z	Height above ground level	
δx	Departure of a variable x	
ϕ_c	Dimensionless concentration gradient	
ϕ_m	Dimensionless wind gradient	
ψ	Water stress	
ψ_c	Integral departure from neutral of ϕ_c	
ψ_m	Integral departure from neutral of ϕ_m	
κ	Thermal diffusivity	[m ² /s]
σ_x	Standard deviation of a variable x	
ν	Kinematic viscosity	[m ² /s]

ON THE USE OF MONITORED AIR CONCENTRATIONS TO INFER DRY DEPOSITION

ABSTRACT. The need for dry deposition data to parallel the wet deposition information obtained in routine monitoring networks is well known, but so are the difficulties. Because there is no simple device capable of measuring the dry deposition rates of small particles and trace gases directly, most current activity is focused instead on the use of a concentration-monitoring procedure. In this method, measurements of the atmospheric concentration (C) of selected chemical species are coupled with evaluations of the appropriate deposition velocity (v_d) so as to yield estimates of the dry deposition rate from the product $F = v_d \cdot C$. Difficulties arise concerning the ability to measure C accurately, and especially regarding the present poor state of knowledge about v_d for many species. Nevertheless, exploratory programs are starting. Some initial responses to the perceived problems are addressed here. Special emphasis is given to the influence of the diurnal cycle, to the way in which various transfer resistances can be inferred from routine data, and to the role of canopy factors (e.g., leaf area index, and wetness) as controlling factors. The intent is not to address questions of a "perfect" field site in a way that would satisfy the requirements of micrometeorological research, but to tailor what is known about micrometeorology to solve problems of dry deposition measurement at real-world sites, such as those of the National Atmospheric Deposition Program, the National Trends Network of the National Acid Precipitation Assessment Program, and areas where research on environmental effects are under way.

1. INTRODUCTION

Concern regarding the deposition of acidic and acidifying substances has led to an awareness of limitations in our ability to monitor dry deposition. At present, there are relatively few programs designed to produce dry deposition flux estimates to augment the wet deposition values routinely produced by programs using standard wet-only bucket samplers. The delay in setting up dry deposition monitoring networks is not due to budgetary or bureaucratic problems; it is a consequence of scientific uncertainty about how to obtain the necessary measurements. The difficulties that arise are well known, and will not be discussed here. Instead, the reader is referred to recent reviews on this subject (e.g., Hosker and Lindberg, 1982; Hicks, 1984; Hosker, 1984), which discuss the factors that influence dry deposition, and provide the overall scientific justification for the methods developed here.

This document summarizes the meteorological component of a monitoring technique to infer dry deposition rates from measurements of air concentrations of chemical species of importance in acid deposition, using parameterizations of deposition velocities to the various surfaces exposed to the atmosphere in given locales.

The definition "dry deposition" requires some discussion. Dry deposition here includes both gas and particle transfer to surfaces exposed to the atmosphere. However, the term is frequently taken to represent all scavenged material that is not collected by a wet-only deposition system and, as such, is extended by some investigators to include aspects of fog interception and other moisture-mitigated mechanisms. In either case, it is different from the dry accumulation (or "dry-fall") collected by some exposed vessels or surfaces constructed of man-made materials.

The limitations of dry-fall collectors and surrogate surfaces are well recognized: they fail to provide data on trace gas or small-particle fluxes that can be related to natural conditions in a convincing manner (q.v. Hicks *et al.*, 1980). However, if it is intended only to measure surface fluxes of large particles that fall under the influence of gravity, then such problems might not be of much concern.

For trace gases and small particles, an alternative sampling system is required. In this context, the "dry deposition" that must be measured is a surface flux similar to the meteorological fluxes of heat, moisture, and momentum. This deposition is a consequence of the same turbulent exchange mechanisms responsible for other meteorological fluxes and is influenced by the local meteorology and a range of surface properties (including physical, chemical, and biological factors). As in the case of the more familiar meteorological fluxes, surface exchange rates of trace gases and small particles can indeed be measured by micrometeorological methods, provided sufficiently sensitive and responsive sensors are available. However, these micrometeorological methods, usually based on covariances or gradients, are sufficiently complicated that routine application in a monitoring network is not yet practical, nor does the prospect of routine application appear likely in the foreseeable future. Consequently, most dry deposition monitoring programs are designed to permit dry deposition to be inferred from other data, with the atmospheric concentrations of the chemical species of interest being essential.

The factor relating dry deposition fluxes to atmospheric concentrations is the so-called deposition velocity, v_d . Although many models and monitoring programs assume v_d to be constant with time and a cardinal property of the chemical species in question, such assumptions are poor approximations of reality. None the less, many models predict long-term concentrations and apply appropriately averaged deposition velocities to evaluate average dry deposition fluxes. Likewise, experimental programs minimize analytical costs by integrating concentration data over days, or even weeks. Thus, appropriately averaged deposition velocities are required to evaluate the desired deposition fluxes.

2. LIMITATIONS AND CONSTRAINTS

Several severe limitations of the methods presently being implemented should be emphasized. First, the techniques are essentially inferential, relying heavily on the accurate measurement of air concentrations and on the evaluation of accurate deposition velocities. Concentration-monitoring techniques suitable for routine use at remote locations are not yet well

developed. However, the dominant limitations are probably those associated with the ability to evaluate appropriate deposition velocities. The knowledge on which any interpretive scheme for deposition can be based is quite limited. Most information on gas transfer either deals with average uptake in laboratory conditions (chambers, wind-tunnels, etc.), or is derived from short-term micrometeorological measurements at carefully selected field sites. Agrometeorology and forest meteorology knowledge concerning water vapor and carbon dioxide exchange is used here as a foundation, but the need for caution remains paramount.

- Laboratory and field studies are either of single plant species or of spatially homogeneous distributions of species. Knowledge is lacking on effects associated with surface heterogeneity.
- No studies have so far addressed the effect of topography. Complex terrain is likely to enhance turbulent transfer, and could possibly modify surface uptake characteristics (especially by soil).
- Real-world knowledge of trace gas exchange is undoubtedly best for water vapor, with an expanding body of knowledge now becoming available for carbon dioxide, ozone, and sulfur dioxide. Some other trace gases (especially nitric acid vapor and nitrogen dioxide) are presently receiving considerable attention. Knowledge of the behavior of other chemical species is limited to laboratory studies.
- Even less is known about particle deposition. Some studies consider particle deposition as a function of particle size. Others focus on the deposition of some particulate species (typically sulfate), without emphasizing the particle size influence. In fact, the technology does not yet exist to consider particulate dry deposition of any specific chemical species in a size-fractionated manner.

Ongoing research programs are addressing these problems. Until their work is successfully concluded, none of the methods addressed here can be advocated with assurance. Indeed, a major task confronting all attempts to "monitor" dry deposition in pilot programs is to assess the magnitude of errors arising from the need to apply poorly-known relationships, and hence to identify areas in which the research effort should be expanded and accelerated. Appendix A summarizes some difficulties associated with factors not yet considered in the present context of routine application at remote locations.

The above comments imply a set of constraints on the applicability of answers derived using the methods outlined here.

- The results will be useful only for locations that have spatially homogeneous vegetation, and where terrain effects are not dominating.
- Values derived will be appropriate for only a limited area surrounding the observing site. The "point measurements" on which the techniques are based imply an "area of applicability" centered on each measurement location, but possibly no larger than 1 km diameter. (This is not seen as a major problem in the context of trends monitoring, since wet deposition suffers similarly.)

- Answers obtained will be best founded for sulfur dioxide and ozone, with nitric acid vapor possibly closely following. Other species cannot yet be addressed with more than minimal confidence, even in the best of circumstances.

Since deposition velocities are complicated functions of meteorological and surface properties which may vary widely with time of day and with season, several other important questions arise. One concerns the accuracy with which we need to know dry deposition fluxes, and how the required accuracies can be achieved. A second concerns the consequences of combining long-term averages \bar{v}_d and \bar{C} when it is known that both quantities are likely to have strong diurnal variability. A third involves the evaluation of appropriate site-specific and species-dependent deposition velocities.

3. REQUIREMENTS FOR RESOLUTION AND ACCURACY

Any dry deposition monitoring program should have the following goals:

1. The time resolution of dry deposition monitoring data should be compatible with existing wet-deposition sampling protocols.

If averages for longer time periods are desired, these averages could be computed by combining data

2. The chemical species to be considered should include the trace gases relevant to acid and acidic precursor deposition (e.g. SO_2 , NO_2 , HNO_3 , NH_3 , and O_3), as well as appropriate particulate anions and cations (e.g. PO_4^{3-} , SO_4^{2-} , NO_3^- , Cl^- , H^+ , Ca^{2+} , Mg^{2+} , Na^+ , etc.).
3. The measurements should be made in a manner leading to the same (or better) statistical confidence in determining spatial and temporal patterns for dry deposition as for wet;
4. The data requirements of effects researchers and modelers should be accommodated as much as possible, either using a specially designed sub-network or by expanding the scope of the trends network.

The difficulties involved in determining spatial and temporal trends in wet deposition data are well recognized. In essence, precipitation is a sufficiently irregular phenomenon that the annual average wet deposition of any species at any specific location cannot be considered to be representative of the relevant spatial average. As a "rule-of-thumb", the error associated with the average annual wet deposition to any site is likely to be in the range 10% - 50%, although admittedly varying widely with location. As knowledge of wet-deposition statistics improves, required accuracies for commensurate dry-deposition measurement can be simultaneously defined. It is obvious, for example, that in some areas time trends might be sufficiently well documented by fewer dry-deposition

stations than wet. However, documentation of important spatial patterns will require more dry stations in source regions than in remote areas.

The trace gas and particle concentration data provided as part of this monitoring effort are also required for other purposes that are of considerable importance in their own right. These include the testing of concentration predictions of long-range transport models, and the requirement for concentrations to help interpret wet deposition data. These needs appear to impose a requirement for more accurate air concentration measurement than would be necessary if the sole aim were the determination of dry deposition. It is apparent, therefore, that air concentrations should be measured as accurately as possible, but with some practical error margin (say $\pm 10\%$), that some margin of error can be tolerated in the evaluation of an appropriate deposition velocity (since even wet deposition data are imperfectly monitored), and that there is benefit in co-locating dry and wet deposition monitoring stations.

4. EFFECTS OF DIURNAL VARIABILITY

The difficulty that arises as a consequence of the diurnal cycles of exchange mechanisms and concentrations is demonstrated schematically in Figure 1. The time records illustrated would yield an average concentration of $C_0/2$ and an average deposition velocity of $v_d/2$, implying an average surface flux of $v_d \cdot C_0/4$. However the records illustrated are temporally arranged to correspond to precisely zero surface flux at all times. The point is that, unless v_d and C are in phase, estimated fluxes inferred from time-averaged v_d and C will be in error.

Consider a specific location at which measurements are made of the long-term average concentration, \bar{C} , with a long-term average deposition velocity, \bar{v}_d , for a given chemical species. The long-term average deposition flux might be estimated as

$$\bar{F}_0 = \bar{v}_d \cdot \bar{C}, \quad (1)$$

whereas in reality it should be computed by integration of instantaneous values:

$$\bar{F}_1 = T^{-1} \int_0^T v_d \cdot C \, dt, \quad (2)$$

where the quantities v_d and C are relatively slowly varying, i.e., they do not contain the high-frequency components of eddy-correlation calculations. If hourly values of v_d and C were available as $v_d(t_j)$ and $C(t_j)$, then an accurate evaluation of the deposition flux could be computed as

$$\begin{aligned} F_2 &= (1/n) \sum_{j=1}^n v_d(t_j) C(t_j) \\ &= \overline{v_d \cdot C} \end{aligned} \quad (3)$$

ATDL-M84/293

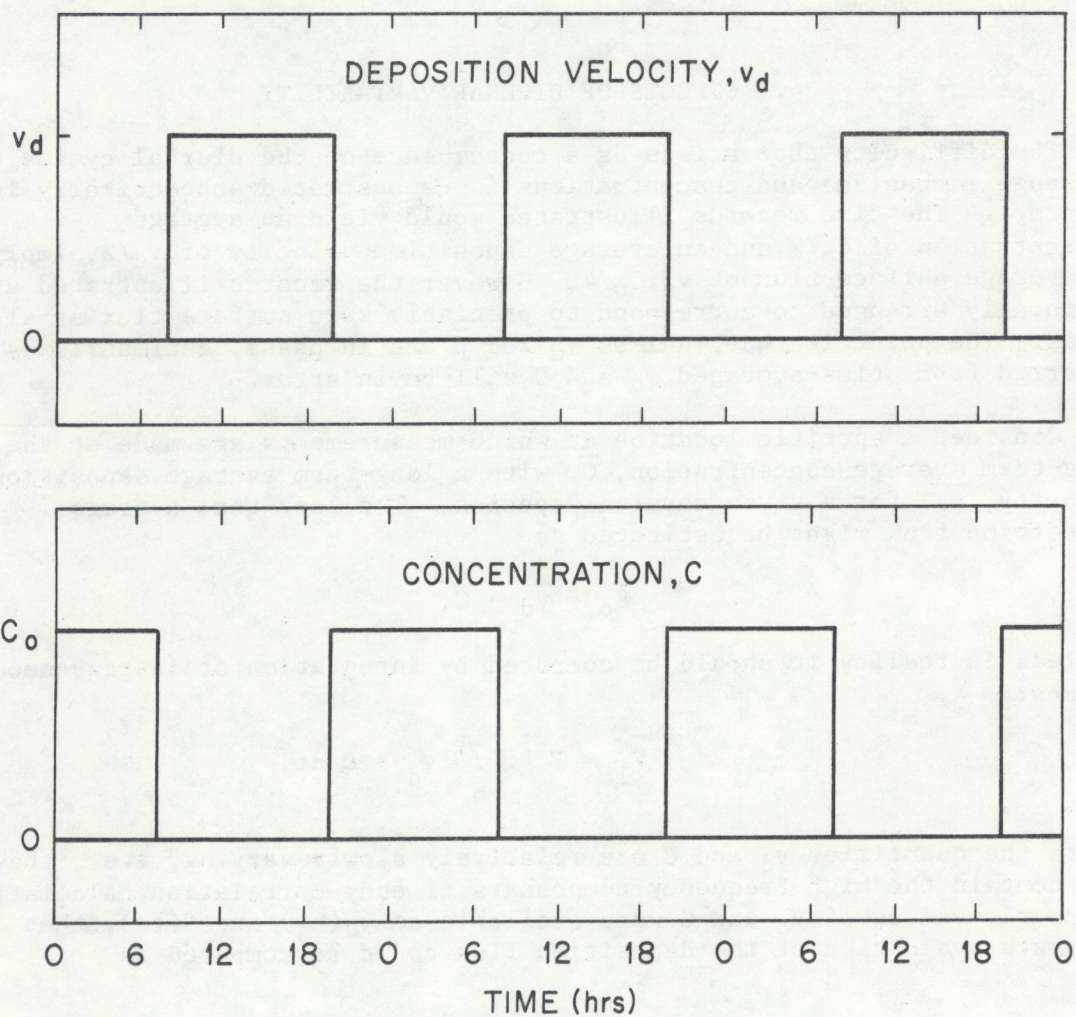


Figure 1.--Hypothetical diurnal cycles of air concentration of a chemical species and the corresponding deposition velocity, selected to demonstrate how the product of long-term averages can differ from the average product.

where n is the number of hours in the period for which F_2 is calculated. It is informative to express v_d as $\overline{v_d} + v_d'$ and C as $\overline{C} + C'$ where the prime indicates a departure from the long-term average indicated by the overbar. Then Equation (3) can be rewritten as

$$\begin{aligned} F_2 &= \overline{v_d \cdot C} + \overline{v_d' \cdot C'} \\ &= F_0 + \overline{v_d' \cdot C'} \\ &= F_0 + \sigma_v \cdot \sigma_c \cdot R_{vc} \end{aligned} \quad (4)$$

where σ_v and σ_c are the standard deviations of v_d and C respectively, and where R_{vc} is the corresponding correlation coefficient. All of these statistics can be computed from hour-by-hour values of v_d and C .

The fractional error involved in applying the approximate form F_0 to estimate the more precise flux F_2 is

$$(F_2 - F_0)/F_0 = (\sigma_v/\overline{v_d}) \cdot (\sigma_c/\overline{C}) \cdot R_{vc}. \quad (5)$$

Here, the quantities $(\sigma_v/\overline{v_d})$ and (σ_c/\overline{C}) will be recognized as the familiar coefficients of variation of v_d and C , computed within the sampling period. In practice, Equation (5) provides a correction that can be applied to the first order approximation represented by Equation (1).

Random noise affecting the evaluation of either C or v_d will not contribute to the correction expressed by Equation (5) because, by definition, such noise will be uncorrelated. Moreover, no sinusoidal variation in either v_d or C will be of importance unless accompanied by a variation with the same frequency in the other, because unlike frequencies are uncorrelated. On these grounds, the correction term expressed by Equation (5) will be dominated by the diurnal cycle. Some exceptions obviously arise, such as when pollutant concentrations themselves influence the deposition velocity, perhaps via some form of biological feedback. These complexities will be avoided here, in order to concentrate on effects associated with the diurnal cycle.

In almost all situations, v_d will display a minimum at night. For ozone, for example, v_d might be about 1.0 cm/s in daytime, yet close to zero at night. The corresponding coefficient of variation is then likely to be high, perhaps close to 1.0. The coefficient of variation associated with air concentrations will usually be substantially smaller, especially in remote areas where the effects of individual plumes and fumigations are small. Figure 2 shows some airborne particle concentration data reported by Johnson *et al.* (1981) for five remote sites in the northeastern U.S.A. Even the Brookhaven (Upton, Long Island, NY), site displays a fairly low magnitude diurnal cycle, even though this particular site is frequently downwind of New York City. Figure 3 illustrates examples of the diurnal variation in ozone concentrations at Oak Ridge, TN. Sulfur dioxide traces for the same period are shown in Figure 4. These examples illustrate several familiar features, such as the effects of plume impaction associated with local sources, and fumigation. Nevertheless, the

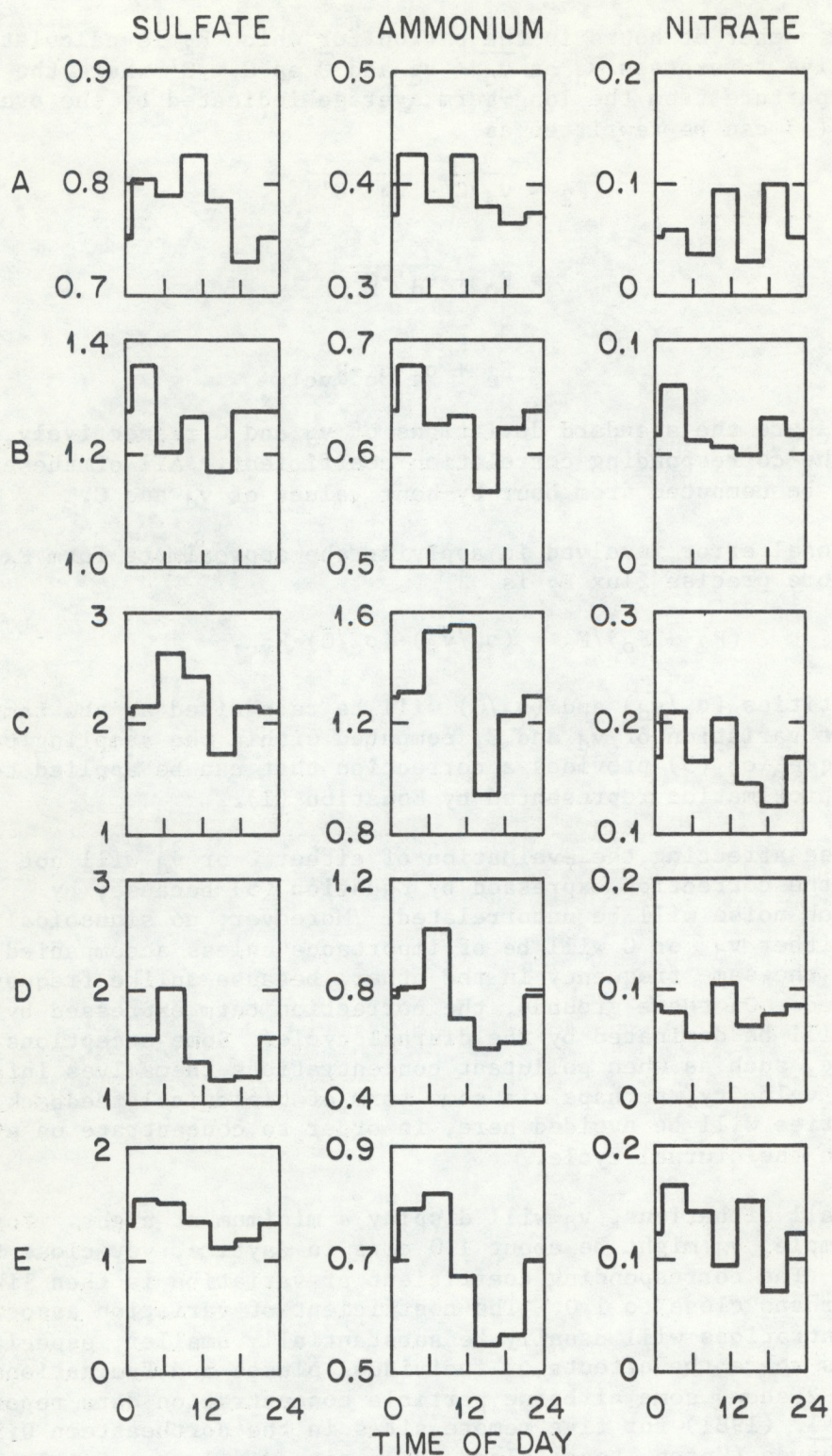


Figure 2.--Average diurnal cycles of near-surface concentrations of sulfate ammonium, and nitrate aerosol, as reported by Johnson et al. (1981) for rural sites located at Raquette Lake, NY (A); Brookhaven National Laboratory, Upton, Long island, NY (B); Rockport, IN (C); Charlottesville, VA (D); and State College, PA (E). Concentrations are all in micrograms per cubic meter.

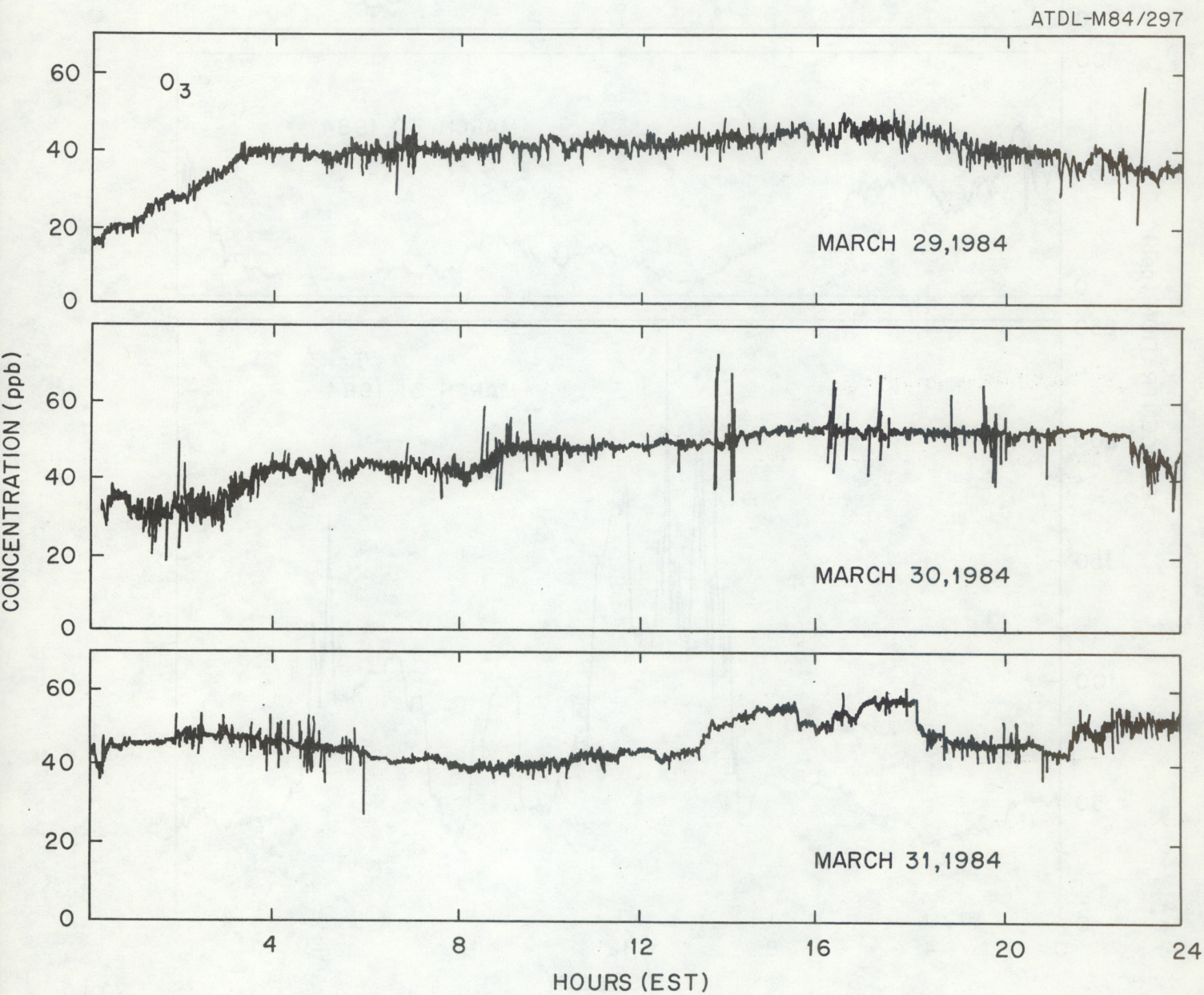


Figure 3.--Ozone concentrations recorded at the Tennessee site of the dry deposition "core" monitoring program, as identified in Figure 5.

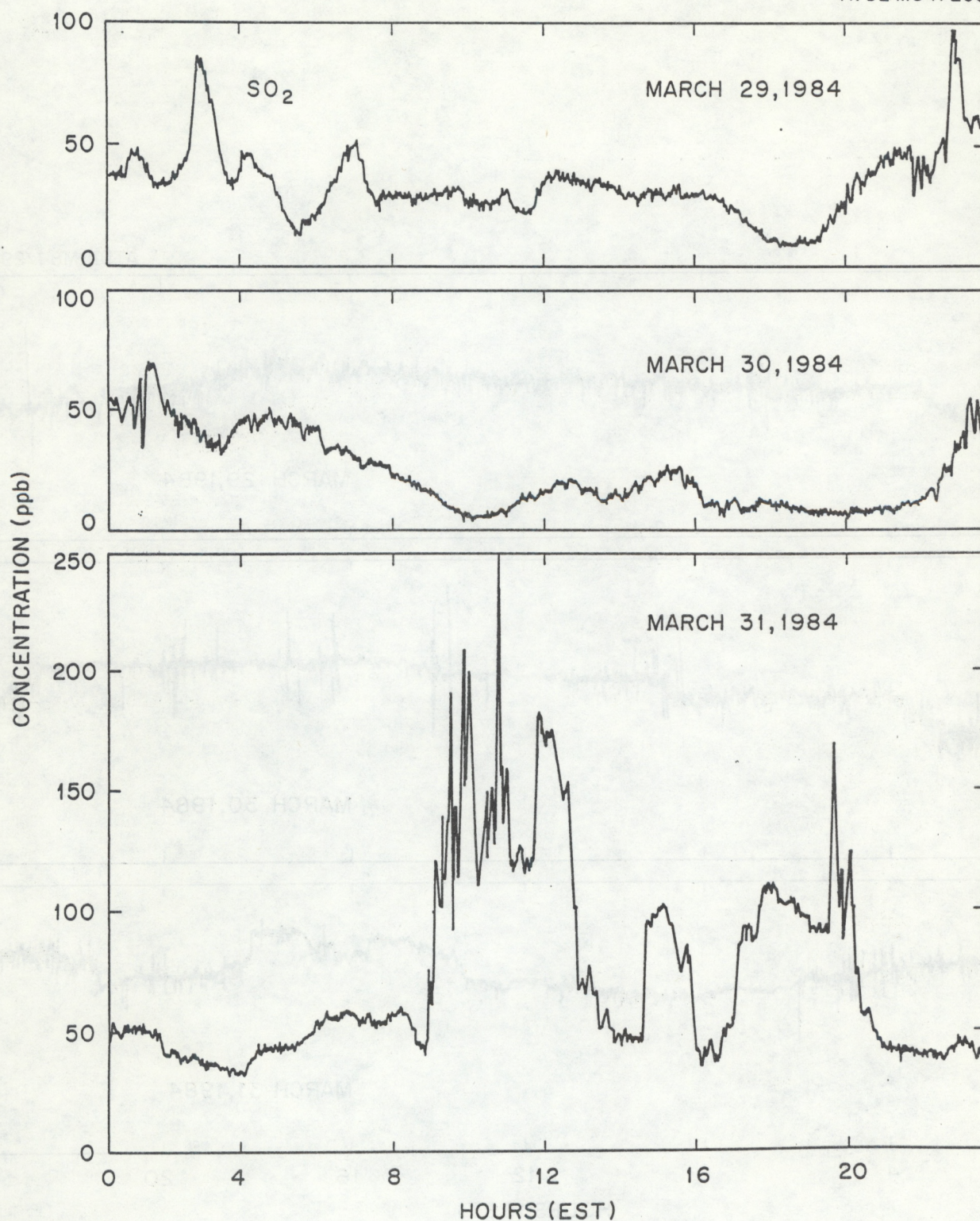


Figure 4.--Examples of sulfur dioxide records obtained concurrently with the O₃ data of Figure 3 at the Tennessee dry deposition "core" monitoring site, as shown in Figure 5. Note the evidence of fumigation episodes on the last day.

correlation coefficient is therefore somewhat uncertain, but might well be near to unity. In general, we might expect the use of time-averaged deposition velocities and concentrations to underestimate, typically by about 20%, the actual average dry deposition rates at remote locations whenever average diurnal concentration cycles and deposition velocity cycles are in phase. When the two cycles are out of phase, an overestimation of similar magnitude will result.

In initial tests of prototype apparatus intended for routine use, alternative methods for addressing the question of the diurnal cycle will be compared. A day/night sampling protocol will be tested in which separate week-long average concentrations will be obtained, one each for days and nights. The dominant diurnal cycle of the deposition velocity suggests that the night-time data are of comparatively little consequence in the context of dry deposition. They are required more for fine adjustment of the daytime-weighted values, and for completion of the record.

The deposition velocity monitoring program discussed here has been designed to permit extensive investigation of such factors as day/night variability. The final output will be a weekly average diurnal cycle of v_d for each chemical species of importance, for all measurement locations, and for every sampling period.

Research programs are also comparing the results of applying the long-term average formulations of Equation (1) and the hour-by-hour direct integration represented by Equation (3). These programs rely on operation of equipment designed for routine use side-by-side with equipment suitable for hour-by-hour measurement of concentrations and meteorological variables required for evaluating deposition velocities. Programs of comparison between the two methods are presently being initiated, with most attention being directed to a small set of "core" research sites located in Illinois, Pennsylvania, and Tennessee (see Figure 5). Figure 6 presents an example of deposition velocities produced by a routinely-operating system of the kind described above. In the particular case illustrated, the pollutant addressed is HNO_3 . The methods used to derive Figure 6 are described in the following sections.

5. EVALUATION OF v_d FROM ROUTINE DATA

A major goal of research programs conducted over the last several years has been to improve understanding of the processes controlling the deposition velocity. A resistance model is generally used to identify and quantify the varied mechanisms involved. Figure 7 illustrates the complexity of the model required to accommodate the natural range of pollutant species and receptor surfaces. It also shows how the processes controlling surface fluxes of these materials can be ordered, quantified, and combined in a logical manner. It should be noted that the present focus is on trace gases and aerosols for which gravitational settling is not greatly important.

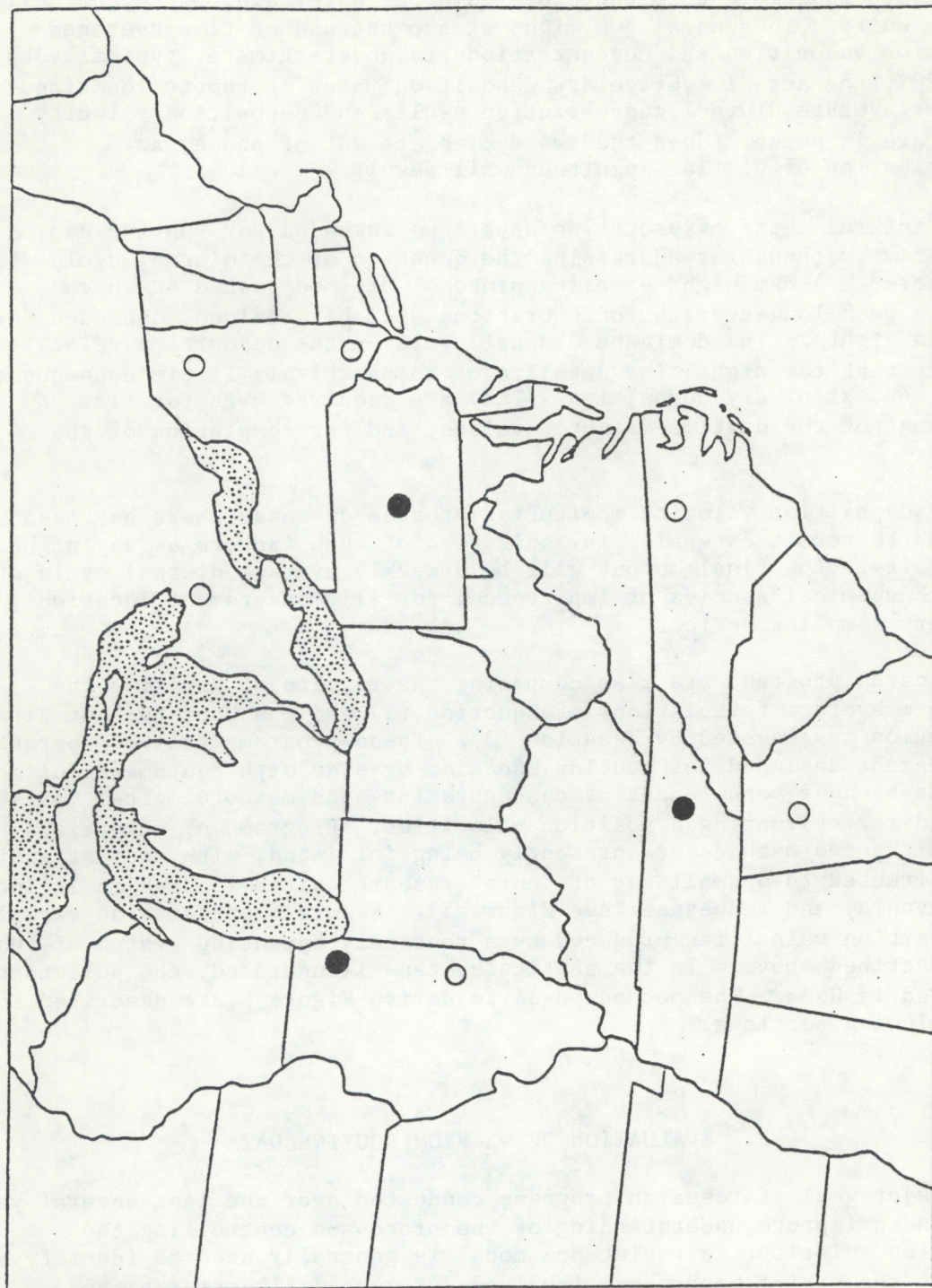


Figure 5.--Sites selected for tests of dry deposition monitoring techniques, with emphasis on the three "core" stations presently in operation (as of June, 1984) at Argonne, Illinois; State College, Pennsylvania, and Oak Ridge, Tennessee.

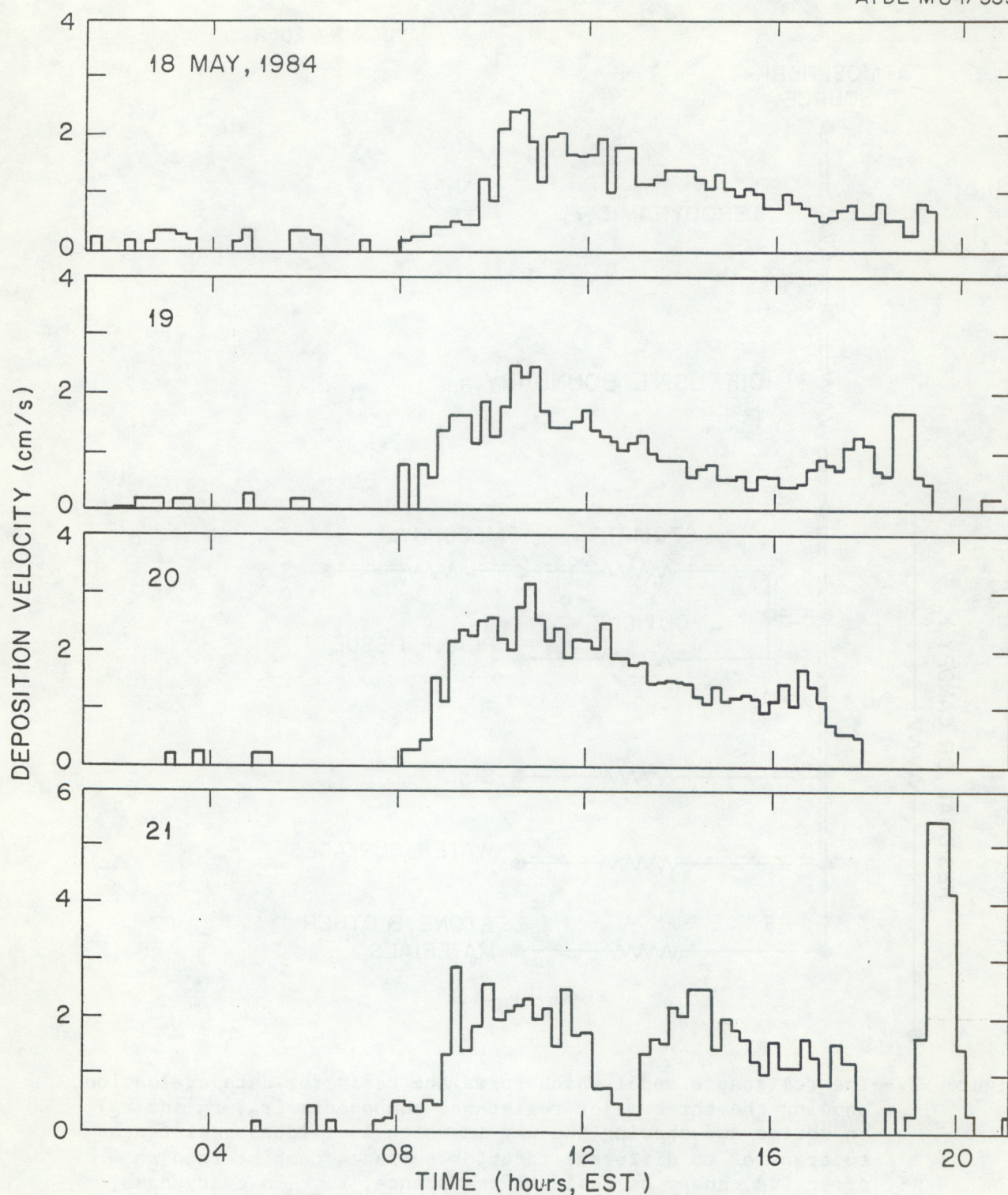


Figure 6.--The variation with time of the deposition velocity for HNO_3 , computed using the methods described in the text during a test of an on-line microprocessor to analyze data from meteorological sensors. Calculations were performed as if the exposure were appropriate for a forest.

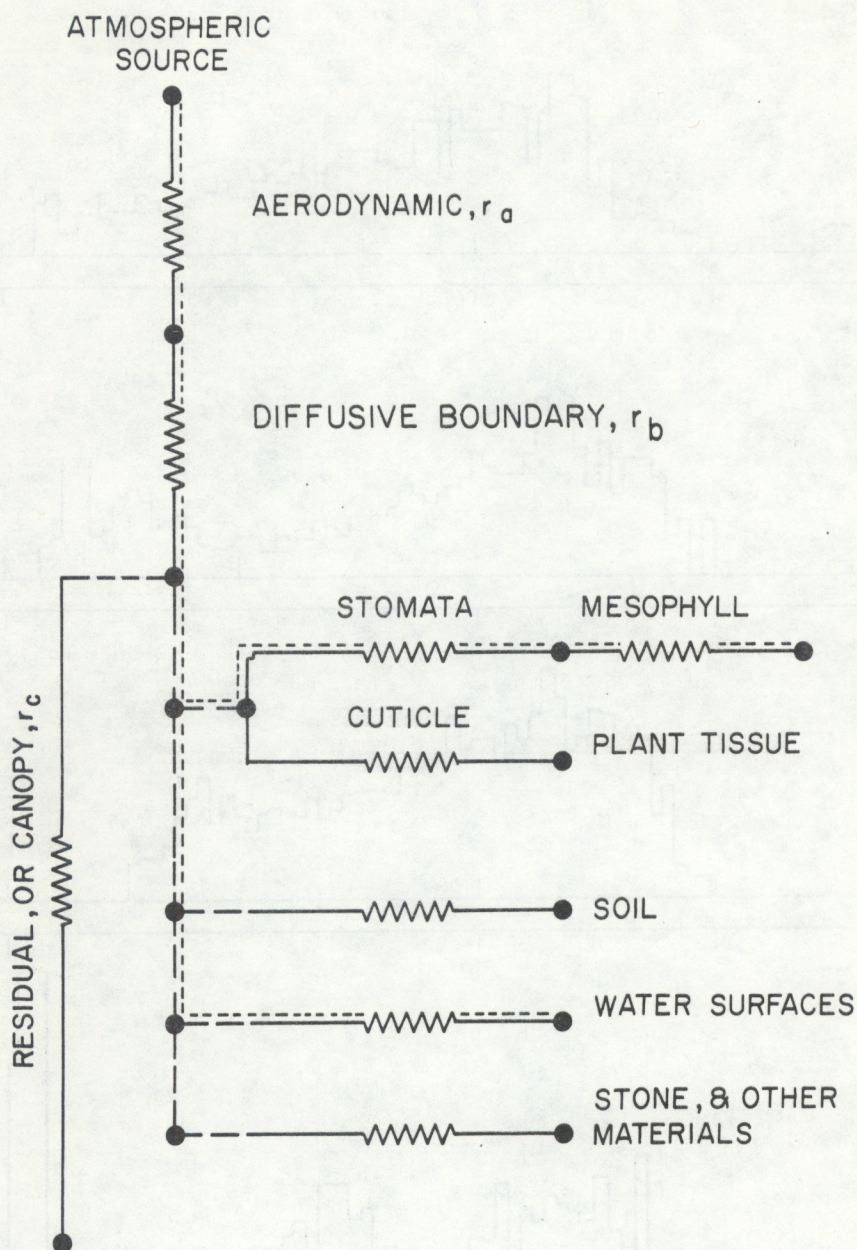


Figure 7.--The resistance model which forms the basis for data evaluation, showing the three major resistance components (r_a , r_b and r_c) in series and showing the way in which individual resistances to transfer to different receptor surfaces combine into an effective canopy as residual resistance, r_c . In every case, major variables affecting individual resistances are identified. As an example of the way different pollutants follow different paths, the dotted line illustrates the probable route associated with SO_2 transfer. In contrast, a highly reactive trace gas like HF or HNO_3 would be expected to deposit quickly via almost all available routes.

A key component of any resistance model of the kind developed here is the way in which effects of surface complexity are accounted for. In general, we might either synthesize surface behavior from detailed knowledge of the behavior of individual surface elements, or parameterize it in terms of quantities that represent average surface characteristics. The conventional micrometeorological approach corresponds to the latter. Surface roughness is typically represented by a single roughness length, z_0 , as in Equation (9) and the effective height of the sink of momentum is represented by a single displacement length, d . The resulting formulations work well, provided they are used to evaluate surface fluxes from observations made well above the surface. Difficulties arise, however, when questions are asked about the distributions of sources and sinks, and about the roles of individual roughness elements. In the present context, the micrometeorological approach will be used. In agricultural meteorology, the concept is sometimes referred to as a "big leaf" approach. In other words, no attempt is made to represent the detailed structure of the surface; rather, the critical factors affecting surface-atmosphere exchange are characterized in terms of the overall process.

An end product of related research activities would be to explain the characterizations of a canopy derived from micrometeorological measurements made well above it, in terms of knowledge of individual components of the surface itself. It is only when such knowledge becomes available that answers will be obtained to questions concerning preferred deposition sites within canopies, and the related location of dominant ecological effects.

5.1 Mathematical Derivation

Consider the flux F of material with airborne concentration C at height z above the zero plane associated with a simple but natural surface (i.e., $z = Z - d$, where Z is height above ground level and d is the zero plane displacement). Following the usual methods of micrometeorology, the flux can be expressed in terms of the local vertical gradient of C as

$$F = -(ku_* z) \cdot (\partial C / \partial z) \cdot \phi_c^{-1}(z/L) \quad (6)$$

Here, k is the von Karman constant (≈ 0.4), u_* is the friction velocity (the root mean covariance between horizontal and vertical velocity components), and ϕ_c is the stability-dependent dimensionless concentration gradient. Following convention, stability is quantified in terms of the Monin-Obukhov length scale L ; the ratio z/L is related to the gradient Richardson number. The function ϕ_c is less than unity in unstable stratification, and greater than unity in stable conditions.

Rearrangement of Equation (6) leads to an integrable form:

$$\begin{aligned} C - C_0 &= - (F/ku_*) \int_0^z [(1/z) - (1 - \phi_c(z/L))/z] dz \\ &= - (F/ku_*) \cdot [\ln(z/z_{oc}) - \psi_c(z/L)] \end{aligned} \quad (7)$$

where ψ_c is an integral form of the departure from neutral of the

dimensionless gradient ϕ_c . At the surface ($z = 0$) or in neutral conditions ($z/L = 0$), $\psi_c = 0$. The roughness length, z_{oc} , is the constant of integration corresponding to the constraint that $C = C_0$ in air in contact with the surface. In practice, the surface concentration is generally not zero since the surface rarely constitutes a perfect sink. The electrical analog illustrated in Figure 7 provides a useful conceptual model. A surface uptake resistance, r_c , can be defined as the ratio C_0/F . An aerodynamic resistance, r_a , can be written as

$$r_a = (1/ku_*) \cdot [\ln(z/z_0) - \psi_c(z/L)] \quad (8)$$

where z_0 is now the familiar roughness length associated with momentum transfer. A remaining resistance

$$r_b = (1/ku_*) \cdot \ln(z_0/z_{oc}) \quad (9)$$

is associated with transfer through the quasi-laminar layer in contact with the surface. This boundary-layer resistance quantifies the way in which pollutant transfer differs from momentum in the immediate vicinity of the surface.

Modeling studies and wind-tunnel investigations agree that r_b is influenced by the diffusivity of the material being transferred. Effects associated with molecular or Brownian diffusivity lie outside the scope of the micrometeorological treatments leading to Equations (7), (8), and (9). However specialized surface transfer models are available to deal with the problem (e.g., Brutsaert, 1975). These models predict a functional dependence of r_b on the Schmidt number, Sc , such that in general

$$r_b \propto (Sc)^\alpha \quad (10)$$

where the exponent, α , is often taken to be $2/3$ but is suspected to vary according to the circumstance.

Many models have also been developed to describe how r_b varies with canopy roughness, classically quantified by the momentum roughness length, z_0 . Figure 8 shows results obtained using two such models, and demonstrates the way in which field observations disagree. As the surface becomes rougher, models tend to predict a monotonically increasing form for the dimensionless resistance $ku_* r_b$, as in Equation (9). However, field studies of sensible heat and water vapor transfer over vegetation yield a substantially different result; $ku_* r_b$ attains a limiting value of about 2. Thus, for the present purposes the quasi-laminar boundary layer resistance r_b is assumed to be given by

$$r_b \cong 2 (1/ku_*) \cdot (Sc/Pr)^{2/3}, \quad (11)$$

where the Prandtl number, Pr , enters to account for the fact that the basic observations are primarily of heat transfer.

The following discussion is intended to show how the important contributing resistances can be derived from basic meteorological (and other) relations. The overall resistance model is a bulk exchange

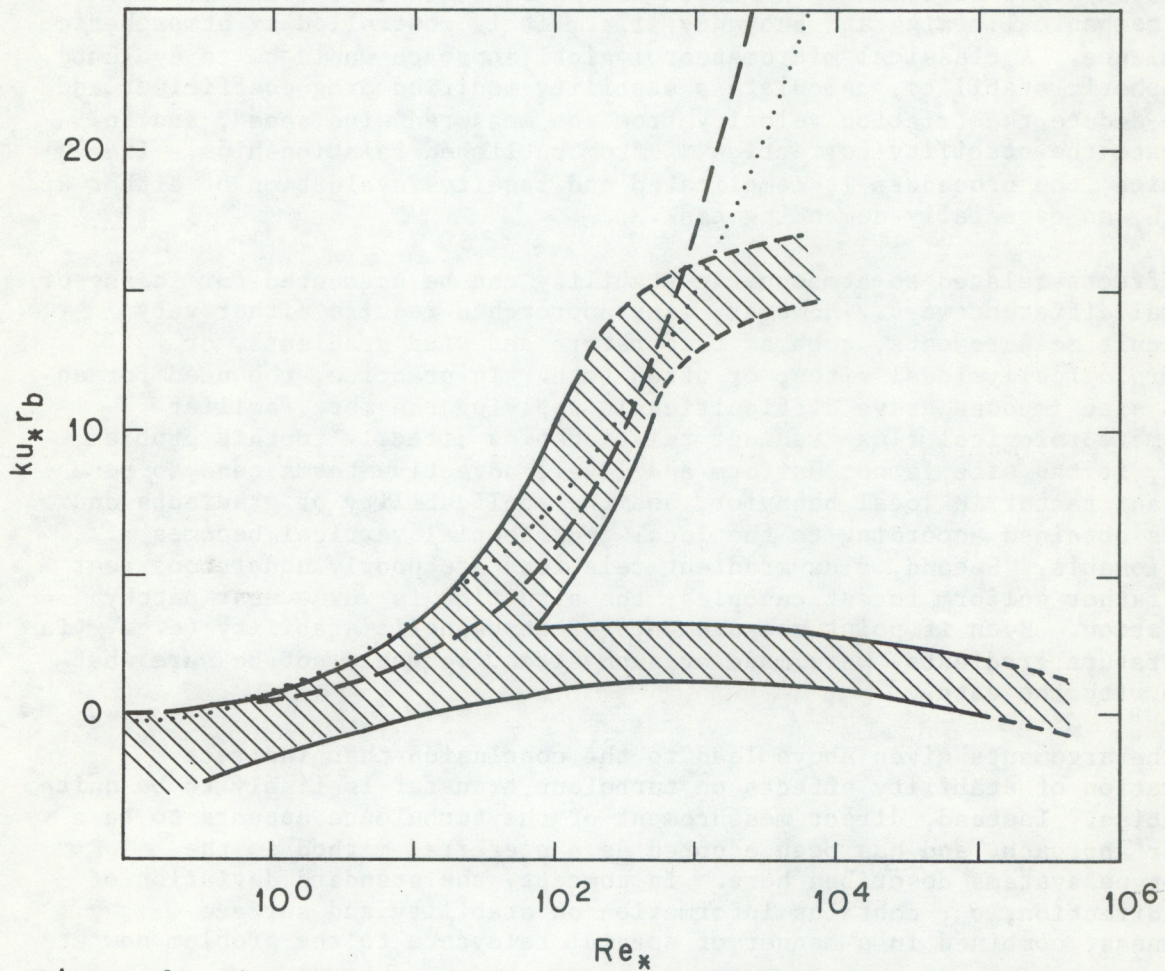


Figure 8. The variation with surface roughness Reynolds number of the boundary-layer resistance indicator, $ku_* r_b$ (see text), as determined for the case of heat transfer. Shaded areas represent field data (as summarized by Garratt and Hicks, 1973) with the upper branch being associated with bluff roughness elements and the lower branch representing vegetation and fibrous roughness elements. The dashed and dotted curves represent formulae derived by Owen and Thompson (1963) and Brutsaert (1975), respectively.

formulation as illustrated in Figure 7. Keeping in mind that the eventual goal is to evaluate rates at which air pollutants are deposited to natural landscapes, questions concerning specific receptors lie outside the present scope and will eventually require the use of a more detailed canopy model than is necessary here. A more detailed canopy model, based on a multi-layered subcanopy simulation of transpiration, is summarized in Appendix B. It is the output of such a model that provides much of the detailed information required to quantify the biological components of the "big-leaf" model represented in Figure 7.

5.2 Evaluating Aerodynamic Resistance, r_a

Aerodynamic resistance (as expressed in Equation (8)) is influenced by both mechanical mixing and buoyancy; i.e., it is controlled by atmospheric turbulence. A classical micrometeorological approach would be to evaluate atmospheric stability, calculate a stability-modified drag coefficient and hence deduce the friction velocity from the measured wind speed, and to estimate the stability correction ψ_c from published relationships. In practice, the procedure is complicated and requires evaluation of either Ri or z/L , an especially demanding task.

Effects related to atmospheric stability can be accounted for in any of several different ways. However, many approaches require either very difficult measurements, such as temperature and wind gradients, or meteorologically ideal sites, or often both. In practice, the need for an ideal site imposes grave difficulties in applying the more familiar micrometeorological flux-gradient relationships directly to this problem. First, if the site is not uniform and level, advective terms tend to be a dominant factor in local behavior, and the applicability of gradients and fluxes obtained according to the local geopotential vertical becomes questionable. Second, flux-gradient relations are poorly understood near even rather uniform forest canopies; the situation is worse near patchy vegetation. Even if point measurements of atmospheric stability (e.g., via temperature gradients) were made at such sites, we would not be sure what to do with the data.

The arguments given above lead to the conclusion that indirect evaluation of stability effects on turbulent transfer is likely to be quite imprecise. Instead, direct measurement of the turbulence appears to be a better approach, and has been adopted as a preferred method in the prototype systems described here. In concept, the standard deviation of wind direction, σ_θ , contains information on stability and surface roughness, combined in a manner of special relevance to the problem now at hand.

Consider measurements of the standard deviation of the horizontal wind direction, σ_θ :

$$\begin{aligned}\sigma_\theta &\cong \sigma_v / \bar{u} \\ &= (\sigma_v / u_*) \cdot (u_* / \bar{u})\end{aligned}$$

$$= (\sigma_v/u_*) \cdot k \cdot [\ln(z/z_o) - \psi_m(z/L)]^{-1} \quad (12)$$

In stable and neutral conditions, it can be assumed as a first-order approximation that $\psi_c(z/L) = \psi_m(z/L)$. Hence, the terms in square brackets can be eliminated between Equations (8) and (12), leading to

$$r_a = (\sigma_v/u_*)^2 \cdot (\bar{u} \sigma_\theta^2)^{-1}. \quad (13)$$

The ratio σ_v/u_* asymptotically approaches a value of about 3.0 in unstable conditions, increasing rapidly after the onset of instability from a neutral value of about 1.9. In neutral and stable stratification, therefore, Equation (13) simplifies to

$$r_a \approx 4 (\bar{u} \sigma_\theta^2)^{-1}; \quad z/L > 0. \quad (14)$$

In unstable conditions (for $-z/L$ greater than about 0.1),

$$r_a \approx 9 (\bar{u} \sigma_\theta^2)^{-1}; \quad z/L < -0.1 \quad (15)$$

An independent evaluation of stability is still needed, even though Equations (14) and (15) contain much of the major relevant information through σ_θ . If net radiation, R_n , is positive, and if σ_θ exceeds some cardinal value A , then conditions can be assumed to be unstable.

Inspection of Equation (12) indicates that A is site-specific because of the functional dependence of σ_θ upon z_o and d . As mentioned above, the ratio σ_v/u_* asymptotically approaches about 3.0 in unstable conditions, increasing rapidly after the onset of instability from a neutral value of about 1.9. A suitable choice for A would therefore be

$$A \approx 0.8 [\ln(z/z_o)]^{-1}, \quad (16)$$

derived by assuming $\sigma_v/u_* \approx 2.0$ in Equation (12), with $k = 0.4$. However, a perfectly-responding sensor to measure the complete turbulence spectrum contributing to σ_θ would be required for such a value of A to be applicable. In practice, a somewhat smaller value must be identified, compatible with the response characteristics of the sensor used. The value $A = 0.17$ (corresponding to $\sigma_\theta = 10^\circ$) is used in the initial phases of this program, and will be refined as further experience is obtained.

5.3 Quasi-laminar Layer Resistance, r_b

There are many different expressions for the resistance, r_b , describing the impedance to turbulent transfer across the quasi-laminar layer in contact with the overall receptor surface. The micro-meteorological forms will be used here, since these have been verified in some detail by field studies conducted over natural terrain. The boundary-layer roughness quantity $\ln(z_o/z_{oc})$, numerically approximated by the factor 2 in Equation (11), expresses the differences between the effective roughness length associated with pollutant transfer and that for momentum, z_o . The Schmidt number, $Sc \equiv \nu/D$, enters as an empirical correction for the molecular (or Brownian) diffusivity of the pollutant

being transferred. Actually, the exponent applied to Sc is not rigorously known. Available information indicates that the exponent is likely to vary from case to case (see Brutsaert, 1979; Hicks, 1984), according to the level of turbulence and the resulting intermittency of the laminar layer in contact with the surface. For most trace gases, the uncertainty associated with the exponent is not critical, but for very slowly diffusing quantities such as aerosol particles, the possible errors become large. This remains a subject for research.

Garratt and Hicks (1973) present data obtained mainly from heat transfer studies which indicate that for natural, vegetated surfaces, the quantity $\ln(z_0/z_{0c})$ should never exceed about 2.0 (see Figure 8). Table 1 lists values of the Schmidt number for a variety of pollutants.

Computation of r_b via Equation (11) requires determination of the friction velocity u_* . In reality, this was an intermediate step in the evaluation of r_a as outlined in Section 5.2. Having determined r_a , therefore, an internally-consistent value for u_* can be derived from the familiar approximation $r_a \approx u/u_*^2$. Given u_* , Equation (11) can be used without further manipulation to determine r_b .

5.4 Surface, or Canopy Resistance, r_c

A key component is the remaining resistance, r_c , associated with the uptake of material by the available natural surfaces. There is a wide range of available pathways for trace gases and for particles as illustrated in Figure 7. For chemically reactive trace gases like HNO_3 , capture at most natural and man-made surfaces is likely to be highly efficient, and hence an assumption $r_c = 0$ will probably be adequate in most cases. Several water-soluble trace gases have been shown to follow similar pathways as water vapor (especially SO_2 , but also less soluble O_3 and NO_2); hence stomatal, mesophyll and cuticular resistances should be considered. For particles, studies of deposition to surrogate surfaces indicate a need to consider characteristics such as stickiness and microscale roughness, which cannot yet be parameterized except in a relatively crude fashion. In many experimental studies, the complexity associated with r_c is sidestepped by the simple expedient of evaluating r_c directly as the residual from the measured total resistance to transfer $R = C/F$, and the known, additive components r_a and r_b . Care must be taken, however, when interpreting published data because some reports consider a residual resistance computed as $R - r_a$, and others consider $R - r_a - r_b$. Only the latter is identical to the canopy resistance r_c discussed here.

Appendix B presents a detailed discussion of how stomatal, mesophyll, cuticular, and soil resistances can be calculated and combined to synthesize the bulk behavior of a vegetative canopy. The detailed resistances are illustrated in Figure 9. The "big leaf" model approach, as applied here, combines gross resistances that correspond to those of a single leaf (schematically shown in Figure 9), equivalent to the canopy as a whole. Thus, a gross mesophyll resistance, r_m , is combined linearly with a gross stomatal resistance, r_s , as if the two were connected in series in an electrical circuit. A gross cuticular resistance, r_{cut} , is visualized as a pathway in parallel with the stomata/mesophyll route. Soil resistance, r_d , is considered as another parallel resistance to transfer to non-vegetative surfaces.

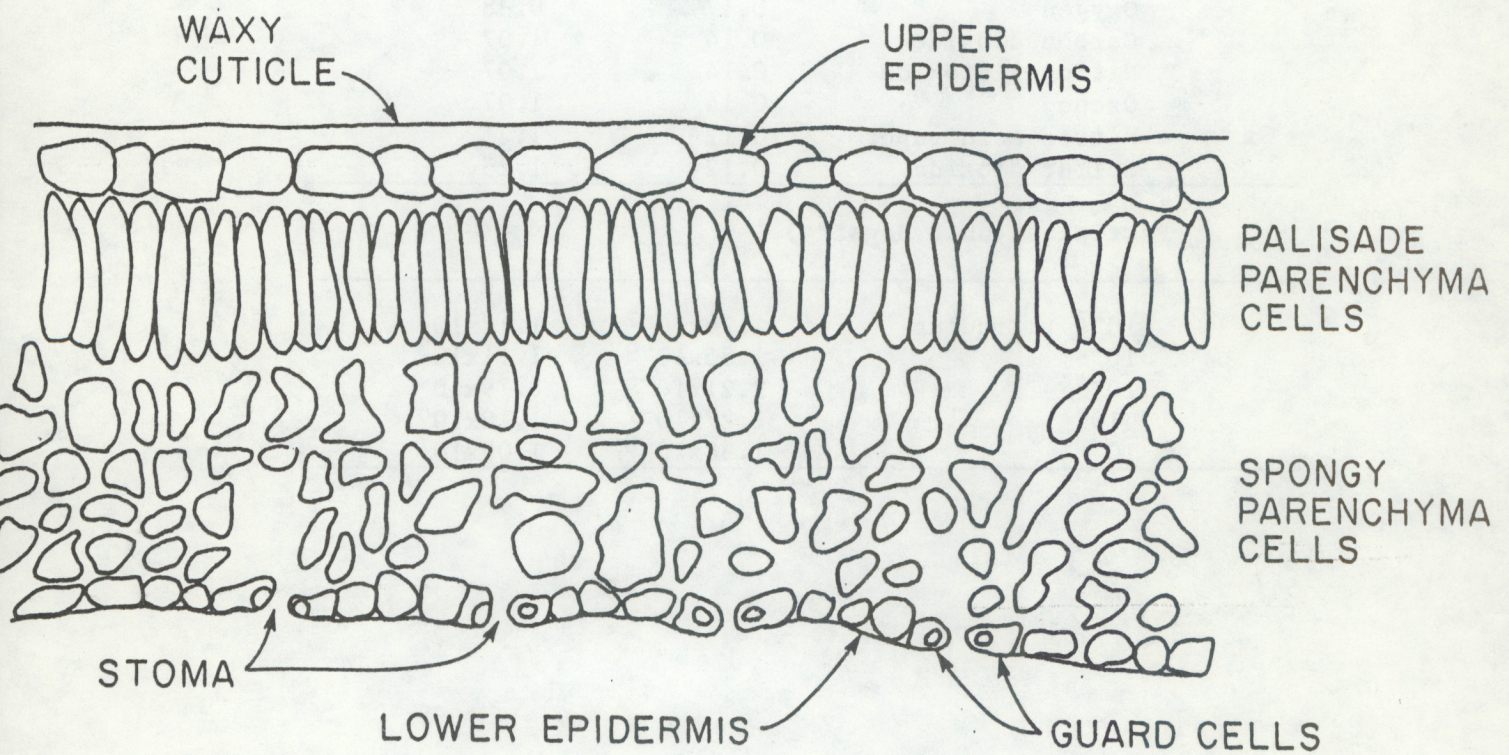


Figure 9.--A schematic illustration of the pathways and processes for transfer between air and plant tissue (following O'Dell et al., 1977).

TABLE 1

Molecular (for gases) and Brownian (for particles) diffusivities (D ; cm^2/s) for a range of pollutants and deduced values of Schmidt numbers (Sc). The viscosity, ν , of air at 20°C is taken to be $0.15 \text{ cm}^2/\text{s}$, at sea level.

	<u>D</u>	<u>Sc</u>
<hr/> Gaseous Species <hr/>		
Hydrogen	0.67	0.22
Water vapor	0.22	0.68
Oxygen	0.17	0.88
Carbon dioxide	0.14	1.07
Nitrogen dioxide	0.14	1.07
Ozone	0.14	1.07
Nitric acid vapor	0.12	1.25
Sulfur dioxide	0.12	1.25
<hr/> Particles (unit density) <hr/>		
10^{-3} μm radius	1.28×10^{-2}	1.17×10^1
10^{-2}	1.35×10^{-4}	1.11×10^3
10^{-1}	2.21×10^{-6}	6.79×10^4
1	1.27×10^{-7}	1.18×10^6
10	1.38×10^{-8}	1.09×10^7

Table 2 presents the formulae from which the present "big leaf" model is constructed. In essence, gross canopy resistance is computed from individual resistivities (i.e., resistances per unit surface area of foliage and other surface features) by application of the canopy's leaf area index (LAI). As is evident in Appendix B, this method should not be expected to be better than a first order approximation.

The leaf area index is defined as the total active area of foliage per unit area of the earth's surface. In some applications, both sides of leaves are counted, but single-sided values are frequently quoted. In rocky terrain, a similar "outcropping area index" could be defined to modify the soil resistance component.

Gross stomatal resistance is taken to be primarily a function of photosynthetically active radiation, I_p , as explained in Appendix B. Effects of water stress, temperature, carbon dioxide, and humidity are quantified by correction factors applied multiplicatively to the gross conductance (the inverse of the corresponding resistance). By definition, each correction factor is in the range 0 to 1.0.

For trace gases that are transferred to plant tissue via the same routes as those associated with water vapor, overall canopy resistance can be computed by applying a Schmidt number correction (outlined in Table 2; see also Appendix B). For SO_2 , NO_2 , and O_3 , the effective daytime resistances calculated in this way are approximately double the water-vapor values computed using Table 2.

Transfer of gases to mesophyll tissue involves absorption into water on cell wall surfaces. If the water were pure, then the Henry's law constant would provide a conceptually satisfying method to account for the differing solubilities of different trace gases. However, the water involved is certainly not distilled or de-ionized; it is enriched with a variety of ions arising from metabolic activity and stomatal uptake. Thus, the question of reactivity arises in a manner which leads directly to the expectation that the final answers will involve a biological species dependence that, as yet, cannot be substantiated by data.

Cuticular resistance is also likely to be influenced by solubility and surface reactivity in ways that have not been identified at this time.

Soil resistance is a matter of equivalent complexity in its own right.

5.5 Canopy Wetness

All of the relations given above were derived for a dry vegetative canopy, with transpiring foliage in a fully-leaved state. Figure 10 shows observed probabilities that a forest canopy is wet, as a function of time of year, including effects of both dew formation and precipitation. The data were generated using an array of wetness sensors (Davis and Hughes, 1970), distributed above and within an oak-hickory forest near Oak Ridge, Tennessee. There is no statistically-significant annual cycle evident in Figure 10. Overall, it appears that the canopy is wet 15% to 20% of the time. The point is that while these data (from a specific forest site over

ATDL-M84/352

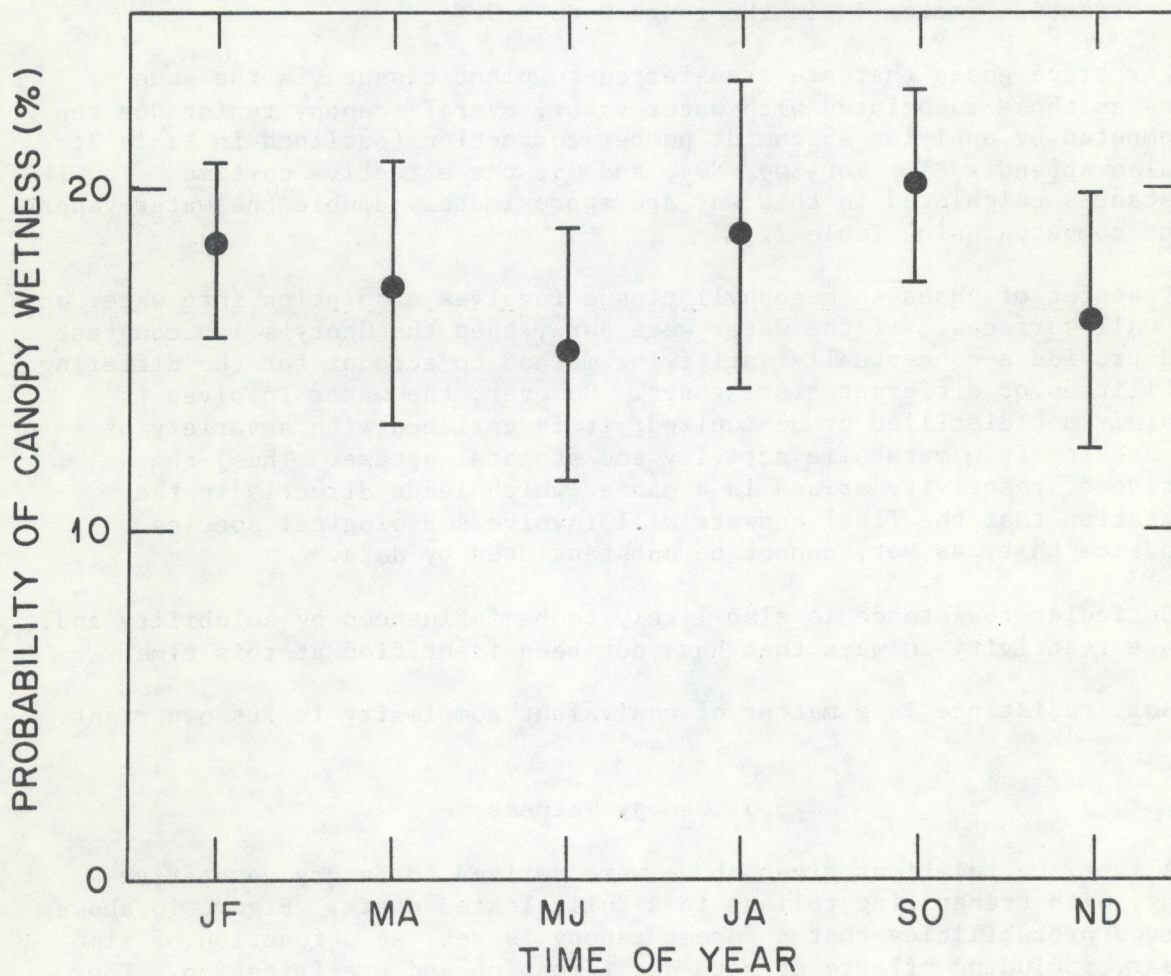


Figure 10. The probability of surface wetness (due to all causes, including dewfall and precipitation) at the forest meteorology research site adjacent to the Walker Branch Watershed, Oak Ridge, Tennessee, over the period from July 1981 to June 1984.

TABLE 2

Summary of relations contributing to first-order evaluation of canopy resistance for particles and trace gases.

Particles: $r_{cp} = r'/LAI.$

Reactive gases:

Dry Canopy: $r_{cg} = [(r'_s \cdot Sc \cdot Pr^{-1} + r'_m)^{-1} + r'_{cut}{}^{-1}]^{-1} / LAI,$

where r'_s is stomatal resistance;

r'_m is mesophyll resistance;

r'_{cut} is cuticular resistance.

For HNO_3 , NH_3 , HF , HCl : $r'_{cut} \approx 0.$

For SO_2 , NO_2 , O_3 : $r'_{cut} = 100 \text{ s/cm}.$

Wet canopy:

For SO_2 , HNO_3 , NH_3 , HF , HCl : $r_{cg} = 0.1 \text{ s/cm}.$

For O_3 , NO_2 : $r_{cg} = 10 \text{ s/cm}.$

the course of only a few years) may not be strictly representative of all canopies, locations, and times, they do indicate that canopy wetness may be a significant boundary condition affecting dry deposition.

Although the consequences of canopy wetness are not well documented, the little available evidence supports expectations. Figure 11 (from Wesely et al., 1978; also see Hicks, 1984) shows the residual, non-aerodynamic resistance, estimated from measured fluxes and concentrations by subtracting the computed aerodynamic resistance, as a function of time of day. The plots show that for ozone (quite insoluble in water) exchange, surface resistance is high while the canopy is wet. For soluble gases, we expect to find very low surface resistances when the canopy is wet.

For the routine monitoring applications of major interest here, wetness detectors are being used to detect surface water. In this first generation of analysis routines, when surface water is detected canopy resistances for ozone are arbitrarily increased to 10 s/cm, and values for sulfur dioxide are assumed to be 0.1 s/cm. Currently available information does not permit a better estimate of the consequences of canopy wetness. The phenomenon is undoubtedly important; research is needed to quantify its effects.

5.6 Effects of Canopy Phenology

Temperate and boreal plant canopies exhibit relatively regular growth and development cycles corresponding to seasonal changes in environmental factors. Since both canopy structure and canopy physiology are affected, such climate-related cyclic (i.e., phenological) factors will affect dry deposition as well. The consequences will be especially pronounced in the cases of annual vegetation such as agronomic crops and perennial plant communities such as prairies and pastures (where only the below-ground portions of the plant persist over winter), and deciduous forests and shrub communities (where the annual cycle of leaf expansion and leaf senescence markedly affects canopy structure).

It is clear from the preceding discussion that changing aerodynamic structure of surfaces will affect dry deposition through changes in z_0 and d , and hence in r_a (Equation 6), and r_b (Equation 10). Canopy resistance, r_c , is also directly affected, because in the extreme case of deciduous perennial plant communities, there are no leaves and hence no stomata, mesophyll, or cuticle to be considered during a significant fraction of each year. Even in the case of plant communities that do not lose leaves in winter, such as conifer forests, the annual solar and growth cycles produce measurable effects on radiative exchange, and presumably on canopy resistance. The implications of the phenology of nondeciduous canopies for dry deposition should not be dismissed without further study.

The phenological dynamics of canopies can also affect dry deposition through temporal changes in stomatal functioning, leaf cuticular roughness (e.g., pubescence), and cuticular waxiness. Insufficient information is available to assess the generality or importance of such suspected cyclical factors. However, it appears that the guard cells that effect the closure of stomata are less effective in many species of plants in controlling

ATDL-M81/102

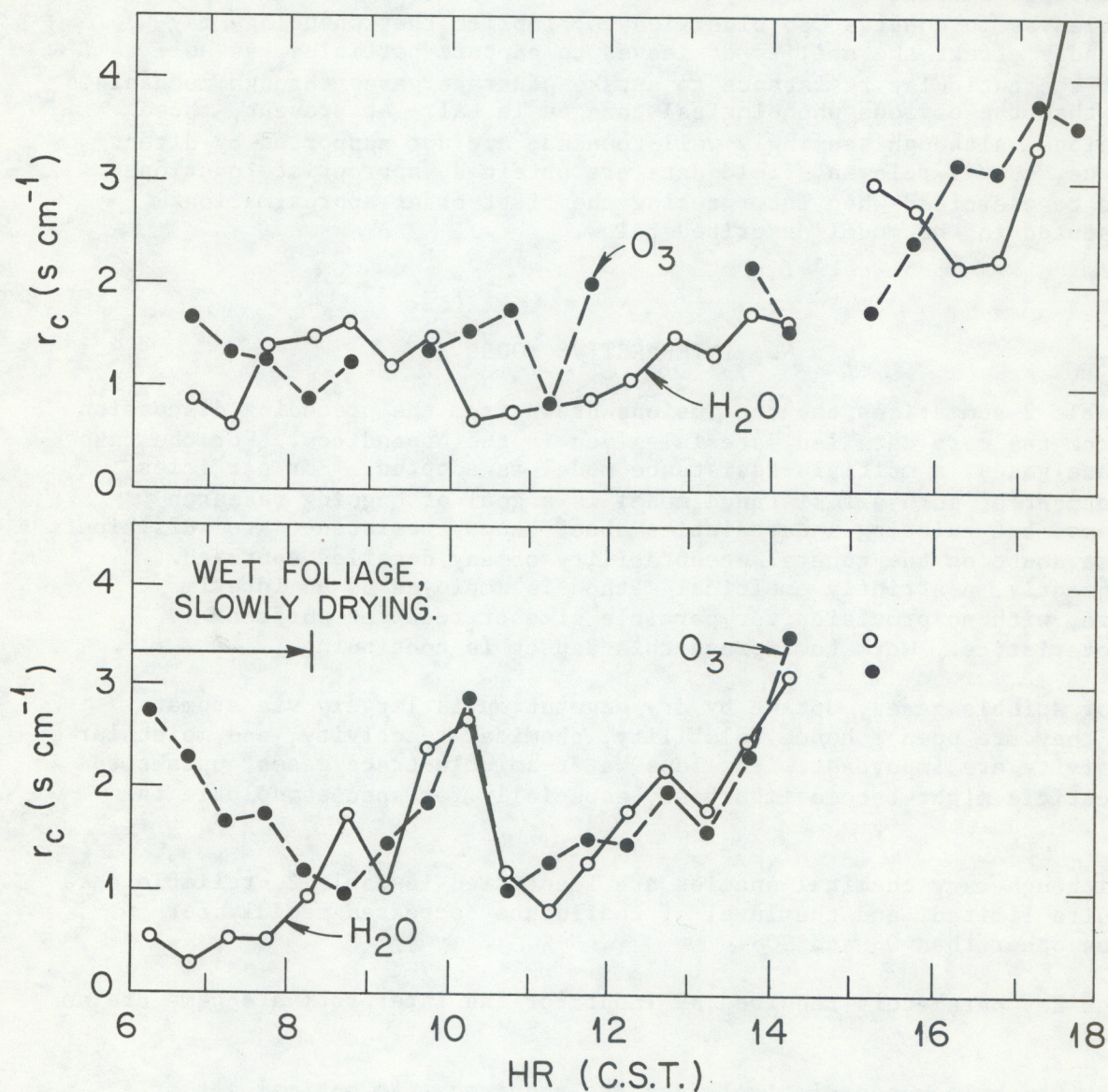


Figure 11.--Residual resistances (i.e., estimated values of r_c) or ozone and water vapor transfer, computed from eddy flux data obtained over a maize canopy (after Wesely et al., 1978). B.l. Vertical distribution of leaf area index for a fully-leaved deciduous forest in summer. The data were obtained at the oak-hickory forest meteorology research site in Oak Ridge, Tennessee.

stomatal aperture during the leaf expansion phase, than when leaves are fully expanded (Brown and Rosenberg, 1970, Burrows and Milthorpe, 1976, Leverenz, et al., 1982, Schulze and Hall, 1982). Thus, in species that produce new leaves throughout the growing season or for a significant fraction thereof (e.g., soybeans, tulip poplar trees), stomata in the youngest leaves may be fully open despite severe water stress, whereas stomata in older leaves will be closed. Furthermore, it is well known that in many plant species, the numbers of stomata, hairs, veins, etc., per leaf do not change as leaves grow. Consequently, the spatial density of these features will decrease with time as leaf area increases. This, coupled with the lack of a waxy or otherwise water-impermeable cuticle in young leaves in contrast to older leaves, implies that phenology may profoundly affect the ability of leaves to capture particles, as well as affect the cuticular resistance to uptake of trace gases through mechanisms other than the obvious phenological changes in LAI. At present, these suspicions, although seemingly well-founded, are not supported by direct evidence. Until relevant field data are obtained, appropriate caution should be exercised when interpreting the first-order approximations represented in the model described below.

6. INTERPRETIVE MODEL

Table 2 summarizes the conclusions drawn from the preceding discussion and from the more detailed material given in the Appendices. For the case of trace gases, a multiple-resistance model is adopted. For particles, development of such a resistance model is a goal of ongoing research programs, but existing uncertainties about canopy resistance are sufficient to cast doubt on the general acceptability of any detailed approach. Consequently, a strictly empirical method is employed as an interim measure, with no provision for particle size or receptor surface characteristics. Work to improve this aspect is continuing.

For soluble gases, uptake by dry vegetation is largely via stomata (when they are open); hence solubility, chemical reactivity, and molecular diffusivity are important. For less water-soluble trace gases, uptake to leaf cuticle might become important (especially for species soluble in waxes).

Although many chemical species are identified in Table 2, reliable data are quite limited, and the level of confidence decreases rapidly for species other than O_3 and SO_2 .

The key parameters required as input for the interpretive scheme are as follows:

- (a) For r_a , only meteorological data are required. An optimal set of information is wind speed, and stability information such as net radiation and the magnitude of σ_θ the standard deviation of wind direction. At high-quality meteorological sites, more precise evaluations of r_a could be obtained by direct measurement of eddy fluxes, or by application of flux-gradient relations to gradient data. It should be remembered, however, that gradient data cannot be easily

interpreted except over smooth surfaces that are horizontal and uniform. Such sites are not the norm.

- (b) For r_b , pollutant characteristics are also important. The Schmidt number is used to modify meteorological evaluations of the quasi-laminar layer transfer resistance based on estimates of the friction velocity derived from wind speed data and knowledge of surface roughness.
- (c) For r_c , knowledge is required of a number of biological factors as well. Stomatal resistance can be estimated from measurements of photosynthetically active radiation (PAR), air temperature, and humidity, coupled with observations of vegetative species and leaf area index. The value of r_c must be modified according to canopy wetness. Effects of water stress and phenology remain to be addressed, but are believed to be important.

Instrumentation suitable for evaluating each of these resistances and for tracking the performance characteristics of the associated chemical devices has been set up (Hosker and Womack 1985) at a small network of test locations identified in Figure 5. At each location, measurements of the following key variables are performed every ten seconds, and average and statistical quantities are calculated every fifteen minutes.

\bar{u} : mean wind speed
 σ_θ : standard deviation of wind direction,
 computed vectorially
T: air temperature
RH: relative humidity
Wn: surface wetness
I: insolation.

Precipitation records will be added to these data (to help detect occasions of severe water stress, and to separate periods when canopies are wet via precipitation, as opposed to dew and fog), and weekly site-operator observations of local surface and canopy conditions are required. These various inputs are analyzed by computer programs, which first search for data inconsistencies or omissions, and, for satisfactory data, then estimate the appropriate transfer resistances. Appendix D presents a listing of the computer code for the resistance program presently in use. This program represents the present state of a continuing research and development effort.

7. CONCLUSIONS

Knowledge of deposition velocities and their controlling factors is not yet adequate to develop a system for evaluating deposition velocities from routine monitoring data with great confidence. However, sufficient

knowledge is present for first-generation interpretive routines to be structured. Preliminary computer codes have been written, and are presently being tested and improved as one component of a pilot dry deposition monitoring program.

Initial operation of this pilot network is focusing on direct evaluation of weekly-averaged atmospheric concentrations. Interpretational difficulties associated with the diurnal cycle are being addressed analytically and by experiment at a second (co-located subset) pilot network of sites where intensive measurement programs are presently underway.

At the time of this writing, the emphasis is on sulfur dioxide and nitric acid vapor, with a secondary interest in ozone and in aerosol particles. Work to include NO and NO₂ is proceeding. In no cases are the appropriate deposition velocities well known.

ACKNOWLEDGEMENTS

This work is a contribution to the National Acid Precipitation Assessment Program, sponsored by the National Oceanic and Atmospheric Administration under programs of Task Group D, Deposition Monitoring. Special thanks are due to Ms. P. Camara of Lowell University for her work on canopy modeling (to be reported in more detail elsewhere), Mr. S. D. Swisher for the canopy wetness data, and to J. D. Womack for his continuing leadership in the experimental programs. Mr. G.-J. Ma of the Atmospheric Environment Monitoring and Research Centre, Nanjing, Peoples Republic of China, developed the instrumentation used to produce the deposition velocities shown in Figure 6.

8. REFERENCES

- Aubuchon, R. R., D. R. Thompson, and T. M. Hinckley, 1978: Environmental influences on photosynthesis within the crown of white oak, Oecologia 35: 295-306.
- Bache, D. H., 1979: Particulate transport within plant canopies. II. Prediction of deposition velocities, Atmos. Environ. 13: 1681-1687.
- Baldocchi, D. D., B. B. Hicks, and P. Camara, 1985: A canopy stomatal resistance model for gaseous deposition to vegetated canopies. In preparation for submission to Atmos. Environ.
- Baldocchi, D. R. Matt, B. A. Hutchison, and R. T. McMillen, 1984: Solar radiation within an oak-hickory forest: an evaluation of the extinction coefficients for several radiation components during fully-leaved and leafless periods. Agric. and Forest Meteorol. 32: 307-322.
- Belot, Y., A. Baille, and J. L. Delmas, 1976: Modele numerique de dispersion des polluants atmospheriques en presence de couverts vegetaux, application aux couverts forestiers. Atmos. Environ. 10: 89-9
- Brown, K. W., and N. J. Rosenberg, 1970: Influence of leaf age, illumination, and upper and lower surface differences on stomatal resistance of sugar beet (Beta vulgaris) leaves. Agron. J. 62: 20-24.
- Brutsaert, W. P., 1975: The roughness length for water vapor, sensible heat, and other scalars, J. Atmos. Sci. 32: 2028-2031.
- Brutsaert, W. P., 1979: Heat and mass transfer to and from surfaces with dense vegetation or similar permeable "roughness". Boundary-Layer Meteorol. 16: 365-388.
- Burrows F. J., and F. L. Milthorpe, 1976: Stomatal conductance in the control of gas exchange. In Kozlowski, T. T. (ed)., "Water Deficits and Plant Growth, Vol. IV", Academic Press, NY, 103-152.
- Davidson, C. I., J. M. Miller, and M. A. Pleskow, 1982: The influence of surface structure on predicted particle dry deposition to natural grass canopies. Water, Air, and Soil Pollut. 18: 25-43.
- Davis, D. R., and J. E. Hughes, 1970: A new approach to recording the wetting parameter by the use of electrical resistance sensors, Plant Disease Reporter 54: 474-478.
- de la Mara, J. F., and S. K. Friedlander, 1982: Aerosol and gas deposition of fully rough surfaces: filtration model for blade-shaped elements. Int. J. Heat Mass Transfer 25: 1725-1735.
- Fisher, M. S., D. A. Charles-Edwards and M. M. Ludlow, 1981: An analysis of effects of repeated short-term soil water deficits on stomatal conductance to carbon dioxide and leaf photosynthesis by the legume Macroptilium Atropureum c. v. Siratro, Aust. J. Plant Physiol. 8: 347-357.

- Garratt, J. R., and B. B. Hicks, 1973: Momentum, heat and water vapour transfer to and from natural and artificial surfaces. Quart. J. Royal Meteorol. Soc. 99: 680-687.
- Hales, J. M., 1983: Parameterization of Removal Mechanisms, Presented at the A.M.S. Conference on Air Quality Modeling of the Non-Homogeneous, Non-Stationary Urban Boundary Layer, Baltimore, MD, 31 October - 4 November, 1983 (available as PNL-SA-11561).
- J Hicks, B. B., M. L. Wesely, and J. L. Durham, 1980: Critique of Methods to Measure Dry Deposition. Workshop Summary. U.S. EPA Report EPA-600/9-80-050 (available from NTIS as PB81-126443) 69 pp.
- Hicks, B. B., M. L. Wesely, J. L. Durham, and M. A. Brown, 1982: Some direct measurements of atmospheric sulfur fluxes over a pine plantation. Atmos. Environ. 17: 2899-1903.
- Hicks, B. B., 1983: Wet and dry deposition of air pollutants and their modeling. In "Conservation of Historic Stone Buildings and Monuments", National Academy Press, Washington, DC, 183-196.
- Hicks, B. B., 1984: Dry deposition processes. Chapter A-7 of The Acidic Deposition Phenomenon and its Effects. U.S. EPA Report 600/8-83-018A, 772 pp.
- ^AHicks, B. B., and R. P. Hosker, Jr., 1983: Dry deposition of air pollutants in an urban environment. Presented at the A.M.S. Conference on Air Quality Modeling of the Non-Homogeneous, Non-Stationary Urban Boundary Layer, Baltimore, MD, 31 October - 4 November, 1983 (available as ATDL Contribution Number 83/15).
- Horn, H. S., 1971: The Adaptive Geometry of Trees. Princeton University Press, Princeton, NJ, 144 pp.
- Hosker, R. P. Jr., and S. E. Lindberg, 1982: Review: atmospheric deposition and plant assimilation of gases and particles. Atmos. Environ. 16: 889-910.
- Hosker, R. P., Jr., 1984: Practical application of air pollutant deposition models -- current status, data requirements, and research needs. In "Air Pollutants and Their Effects on the Terrestrial Ecosystem" (A. H. Legge and S. V. Krupa, eds.), John Wiley, NY. In press.
- Hosker, R. P. Jr., and J. D. Womack, 1985: Prototype Meteorological Monitoring and Filterpack Sampling Systems for Dry Deposition Measurement, NOAA Technical Report. In preparation.
- Jarvis, P. G., 1971: The estimation of resistances to carbon dioxide transfer, pp. 566-631 in "Plant Photosynthetic Production: Manual of Methods" (Z. Sestak, J. Catsky and P.G. Jarvis, eds.), Junk, The Hague.

- Jarvis, P. G., 1976: The interpretation of the variations in leaf water potential and stomatal conductance found in canopies in the field. Phil. Trans. Royal Soc., London, B 273: 593-610.
- Jarvis, P. G., W. R. N. Edwards, and H. Talbot, 1981: Models of plant and crop water use. In Mathematics and Plant Physiology (D. A. Rose and D. A. Charles-Edwards, eds.), Academic Press, New York, 151-197.
- Johnson, S. A., R. Kumar, P. T. Cunningham, and T. A. Lang, 1981: The MAP3S Aerosol Sulfate Acidity Network: a Progress Report and Data Summary. Argonne National Laboratory Report ANL-81-63, 139 pp.
- Leverenz, J., J. D. Dean, E. D. Ford, P. G. Jarvis, R. Milne and D. Whitehead, 1982: Systematic spatial variation of stomatal conductance in a sitka spruce plantation. J. Appl. Ecol. 19: 835-851.
- Liss, P. S., and P. G. Slater, 1974: Flux of gases across the air-sea interface. Nature 247: 181-184.
- McConathy, R. K., S. B. McLaughlin, D. E. Reichle, and B. E. Dinger, 1976: Leaf Energy Balance and Transpirational Relationships of Tulip Poplar (*Liriodendron Tulipifera*). ONRL Environmental Sciences Division Pub. No. 918, 109 pp.
- O'Dell, R. A., Mansoor Taheri, and R. L. Kabel, 1977: A model for the uptake of pollutants by vegetation. J. Air Pollut. Contr. Assoc. 27: 1104-1109.
- Owen, P. R., and W. R. Thompson, 1963: Heat transfer across rough surfaces. J. Fluid Mechanics 15: 321-334.
- Peters, L. K., 1984: Gases and their precipitation scavenging in the marine atmosphere. In Air-Sea Exchange of Gases and Particles (W. G. N. Slinn and P. S. Liss, eds.), D. Reidel, Dordrecht, Holland, 173-240.
- Rodriguez, J. L., and W. J. Davies, 1982: The effects of temperature and ABA on stomata of *Zea Mays* L, J. of Expt. Botany 33: 977-987.
- Russell, I. J., C. E. Choquette, S.-L. Farg, W. P. Dundulis, A. A. Pao, and A. A. P. Pszenny, 1981: Forest vegetation as a sink for atmospheric particulates: quantitative studies on rain and dry deposition. J. Geophys. Res. 86: 5347-5363.
- Schulze, E. D., and A. E. Hall, 1982: Stomatal responses, water loss, and CO₂ assimilation rates of plants in contrasting environments. In: O. L. Lange, P. S. Nobel, G. B. Osmond, and H. Ziegler, Encyclopedia of Plant Physiology, New Series, Vol. 12 B: Physiological Plant Ecology II. Springer-Verlag, Berlin, pp. 181-230.
- Slinn, W. G. N., 1982: Predictions for particle deposition to vegetative canopies. Atmos. Environ. 16: 1785-1794.

- Turner, N. C., S. Rich and P. E. Waggoner, 1973: Removal of ozone by soil. J. Environmental Quality 2: 259-267.
- Unsworth, M. H., 1980: The exchange of carbon dioxide and air pollutants between vegetation and the atmosphere. Chapter 7 in Plants and their Atmospheric Environment (J. Grace, E. D. Ford and P. G. Jarvis, eds.), Blackwell Scientific Publications, Boston, MA, pp. 111-138.
- Wesely, M. L., J. A. Eastman, D. R. Cook, and B. B. Hicks, 1978: Daytime variation of ozone eddy fluxes to maize. Boundary-Layer Meteorol. 15: 361-373.
- Wesely, M. L., and B. B. Hicks, 1977: Some factors that affect the deposition rates of sulfur dioxide and similar gases on vegetation. J. Air Pollut. Control Assoc. 27: 1110-1116.
- Wesely, M. L., D. R. Cook and R. L. Hart, 1983: Fluxes of gases and particles above a deciduous forest in wintertime, Boundary-Layer Meteorol. 27: 237-255.

Appendix A: Some Special Considerations

Integrations of Detailed Information.

Most knowledge concerning air-surface exchange of trace gases and particles originates either from laboratory studies in controlled conditions, or from field experiments at locations selected to address specific questions. Existing knowledge covers a wide range of surface conditions, pollutant species, and meteorological situations, but with wide gaps over which it is now necessary to interpolate.

It is useful to consider a range of required information in the form of a three-dimensional array, ordered according to the number of chemicals (I), the number of surface conditions of relevance (J), and the number of meteorological exposure conditions (K). Although no ordered lists have been constructed that would enable I, J, and K to be enumerated, we might expect each to be of the order of twenty, even after ordering so that only important factors are included. Thus, the array of importance might be expected to contain about 8,000 elements, of which available information can probably address directly fewer than 100.

It is obvious that the need for more knowledge is great, and that current methods for addressing natural situations in real-world surroundings should be considered with caution. It is also obvious that few landscapes will be so uniform that they will be characterized by a single array element. Similarly, it is probable that some species will have to be considered in conjunction with others, taking chemical interactions into account. Thus, in any realistic situation we are likely to be forced to consider some indistinct "volume" within the three-dimensional matrix described above, rather than any single element of that matrix.

Methods by which averages can be constructed using the piece-by-piece knowledge that is presently available are not always obvious. Some guidance can be obtained from meteorological studies, however. The agricultural need to assess evaporation from a mosaic of surfaces with differing surface exchange characteristics has resulted in an extensive research effort which has continued for decades. A first order approach is now obvious: evaluate evaporation rates from each of the individual areas, given the controlling properties appropriate for each, and then integrate the answers on an area-weighted basis. While this technique is quite satisfactory in many circumstances, it fails to take into account the striking effects associated with discontinuities, as (for example) between ploughed fields and forests. In this context, an important factor would seem to be the number of "important" edges within any area of interest, as well as the total area distribution of the major contributing surface types. What constitutes an important discontinuity remains to be evaluated. The same arguments apply to pollutant deposition, for which the level of understanding is substantially lower, and uncertainties are magnified.

From the viewpoint of deposition monitoring, these problems can be minimized by carefully arranging monitoring sites to be in "representative"

locations where surface discontinuities are not a dominating feature of the local landscape. Given a network of such locations, the question then arises as to the method by which the data obtained can be interpolated, in order to derive spatial averages such as are required, for example, to test the prediction of numerical models. As yet, no such technique has been proven.

Adaptive Ecological Characteristics of Plant Communities

Evolution has been said to proceed to fill vacant ecological niches. At the same time, no two species can occupy the same niche; consequently, species survival requires evolutionary adaptations which reduce interspecies competition to tolerable levels by niche differentiation, i.e., specialization. The nature of the adaptive characteristics of the plant species making up plant communities may be of some importance to dry deposition, especially in non-man-dominated landscapes. Consider a simplistic and extreme situation found in the forests of Southern Appalachia. Tulip poplar, a seral tree species, commonly occurs on north-facing slopes, in sheltered coves, and in stream bottoms throughout this region. Being adapted to such moist sites, this species exhibits little stomatal control over transpirational water loss; its stomata tend to remain open despite severe water stress (McConathy et al., 1976). If leaves permanently wilt during periods of drought (as they commonly do), they are shed, and when rains replenish the soil moisture, a new flush of leaves is immediately produced.

The much drier ridge tops and south-facing slopes of this region are forested by tree species adapted to drier sites. A common adaptive characteristic of the dry site species such as yellow pines or oaks and hickories is more effective stomatal control of transpiration. When dry site-adopted species become stressed, the stomata begin to close. Generally, this reduces water loss to tolerable levels, and the leaves are not shed until autumn. In any event, leaf buds are not present in most of these species throughout the year. Thus, only one flush of leaves is produced each year and if defoliation occurs, the canopy remains defoliated until the following spring. Thus, the bulk canopy resistance r_c , which is a strong function of stomatal resistance r_s , for forests in this region will be controlled to some degree by the nature of the site adaptations of the tree species making up particular forest stands.

Effects of ecological succession upon longer-term trends in dry deposition may need to be considered as well. Differences in leaf anatomy and photosynthetic physiology appear among the species appearing in the various successional stages (Horn, 1971). Because of the relationship between canopy structure and aerodynamic characteristics such as z_0 and d , long-term successional changes in canopy architecture may also be expected to cause long-term, subtle changes in turbulent exchange, with consequent effects upon r_a , r_b , and r_c .

Snow and Liquid Water Surfaces

The emphasis of the material presented here is vegetated surfaces. However, the case of deposition to a snowpack is of special interest because of the effects apparently associated with melt. There is considerable information on particle deposition to snow, and a rapidly expanding body of data on sulfur dioxide transfer. Much of this information has been reviewed by Hicks (1984). Several fundamental conclusions have been used to guide the methods adapted as an interim measure for formulating deposition to snow and water surfaces.

- Ozone is essentially insoluble in clean water regardless of its phase. Hence, ozone surface resistance of clean snow surfaces is taken to be very large.
- Sulfur dioxide is soluble in water if the pH is not less than 3.5.
- Nitric acid vapor and gaseous ammonia will be removed rapidly and efficiently upon contact with the surface; hence surface resistance of water for these compounds is taken to be zero.
- Open water surfaces are often quite smooth, whether liquid or solid. Hence, the familiar particle-size dependence of particle deposition is likely to be especially important. Effects of breaking waves are presently disregarded.
- Atmospheric stability is likely to take extreme values over water surfaces, because of their relative smoothness. Thus, accurate assessment of aerodynamic resistance will be particularly important. For the present, the residual, or canopy, resistance term in Figure 7 is assumed to be modified by a pathway parallel to vegetation, having resistance characteristics as indicated above.

Urban Areas

The presence of large areas of stone, pavement, metal, and other construction materials makes urban areas exceedingly difficult to deal with, the complexities arising have been reviewed by Hicks (1983), Hales (1984), and Hicks and Hosker (1984). Highly site-specific localized flow patterns and regions of turbulence and vorticity further complicate the problem. During the preliminary operation of the pilot dry deposition monitoring network, no stations are being set up in urban areas. The subject is under continuing scrutiny of this writing.

Appendix B: Modeling Trace Gas Exchange in Canopies

Introduction

The canopy transfer resistance, r_c , represents the residual resistance after turbulent and laminar effects are taken into account. Agricultural and forest meteorologists have focused on the question of what determines r_c , with traditional emphasis on water vapor, heat, and carbon dioxide, but recently concern has been extended to gaseous pollutants (e.g. Unsworth, 1980). As starting points, we refer to summaries presented by Jarvis (1976) and Jarvis et al. (1981).

Special caution must be exercised with respect to nomenclature. Many specialists quantify resistances associated with biological pathways (via stomata and leaf cuticle, in particular) in terms of a biological resistance to transfer, which differs in concept from that considered here. The difference is easy to understand: field experimentalists evaluate the biological resistances as effective resistances per unit area of foliar surface, whereas in the present context we are mainly interested in the integrated consequences of these resistances expressed per unit horizontal area of the earth's surface. The link between the two is the leaf area index (LAI), and its equivalents that refer to other components of the biomass. However, extension of detailed knowledge of the behavior of individual canopy element surfaces to a complete canopy is far from trivial. In essence, this task constitutes a major goal of the specialties of agrometeorology and forest meteorology. For some properties (e.g. heat and water vapor), synthesis of complete canopy behavior can be accomplished with some confidence. For other quantities (especially particles), resolution of the problem still appears quite distant (see Appendix C). We proceed, therefore, with awareness that the methods presently advocated are best suited to trace gas transfer, and to canopies with small LAI.

To avoid confusion, primes will be used to identify resistances expressed in terms of a unit area of foliar surface (i.e., biological resistances). In accordance with canopy-modeling convention, the individual conductances corresponding to the inverses of the various resistances will be identified by the symbol g .

Stomatal resistances, r'_s

Transfer through stomata is by diffusion; thus, an inverse dependence of stomatal resistance on molecular diffusivity of trace gases is normally accepted (see Jarvis, 1971, for example). In general, stomatal resistance depends on the incident photosynthetically active radiation (I_p):

$$\begin{aligned} r'_s &= r'_{sm} (1 + (b/I_p)) \\ &= (g_s)^{-1} \end{aligned} \tag{B.1}$$

where r'_{sm} is a minimum value which varies with the plant species, and

b is an empirical constant (Burrows and Milthorpe, 1976). Table B.1 summarizes the results of experimental investigations of components of Equation B.1.

Equation B.1 provides a means to evaluate stomatal resistance, expressed per unit leaf area, assuming the vegetation is freely transpiring. Jarvis (1976) provides relations for modifying the effective stomatal conductance to account sequentially for effects of water stress, air temperature, and air humidity. In each case, extreme conditions can have a drastic influence on stomatal resistance. The literature survey and analyses summarized by Jarvis suggest a linear reduction of stomatal conductance ($g_s = 1/r'_s$) with increasing atmospheric vapor pressure deficit $\delta e [\equiv e_s(T) - e]$, where $e_s(T)$ is the saturated water vapor pressure at air temperature T, and e is the actual atmospheric vapor pressure (note that the relative humidity $RH \equiv e/[e_s(T)]$). To account for this reduction, a multiplier

$$f_e = 1 - b_e \cdot \delta e \quad (B.2)$$

is defined, where b_e is a constant indicative of the response of a given plant species. The multiplier f_e is then applied to the conductance $g_s [(r'_s)^{-1}]$ calculated from Equation B.1.

Plant water stress can be quantified in thermodynamic terms using the leaf water potential (ψ). Stomatal resistance is relatively independent of ψ , until ψ drops below a threshold value. Below the threshold value, r'_s increases rapidly. The influence of ψ on g_s can be incorporated using a "discontinuous switch" model (Fisher et al., 1981).

$$f_w = 1, \text{ if } \psi > \text{threshold}, \quad (B.3a)$$

$$f_w = a \cdot \psi + b, \text{ if } \psi < \text{threshold}, \quad (B.3b)$$

where a and b are constants.

Absolute temperature effects can be introduced with a further modifying factor

$$f_T = \{[(T-T_\ell)/(T_o-T_\ell)] \cdot [(T_h-T)/(T_h-T_o)]\}^{b_T} \quad (B.4)$$

where

$$b_T = (T_h - T_o) / (T_h - T_\ell).$$

Here, T_h and T_ℓ are the species-dependent higher and lower temperature extremes at which stomata no longer open (typically 40°C and 5°C, respectively, but see Table B.2), and T_o is the temperature at which stomatal exchange is optimized (typically 25°C). Hence b_T is typically about 0.4.

TABLE B.1

Results of experimental studies, as summarized by Baldocchi et al., (1985), of the relationship between stomatal resistance and photosynthetic radiation intensity, I_p . A relationship of the general form of Equation B.1 is assumed.

Crop	r'_{sm} ($s\ m^{-1}$)	b (W^{-2})
Soybean	65	10
Oak	145	22
Maize	100	66
Spruce	232	25

TABLE B.2

Characteristic temperatures ($^{\circ}C$) associated with the stomatal resistance of different species, as specified in Equation B.4.

Species	T_o	T_h	T_l
Maize ¹	25	45	5
Spruce ²	9	35	-5
Fir ²	20	45	-5
Oak ³	10	45	25

References:

1. Rodriguez et al. (1982)
2. Jarvis (1976)
3. Aubuchon et al. (1978)

A final modifying factor concerns CO₂ levels. Since all of the applications for the present analysis involve the unmodified atmosphere, existing ambient CO₂ concentrations will be assumed. The well-documented trend with time and the seasonal oscillation in ambient CO₂ will not be considered here, since they are too small to have consequences comparable to those of the factors considered above.

The modifying factors f_e , f_w , and f_T all lie in the range $0 \leq f \leq 1.0$. Their effect is to cause an adjustment to the basic relationship for conductance as represented by Equation B.1:

$$g_s = r_{sm}'^{-1} (1+b/I_p)^{-1} \cdot f_e \cdot f_w \cdot f_T \quad (B.5)$$

Extension to a canopy is not trivial. A common expedient is to apply the leaf area index (LAI) as an additional correction factor. Before considering this subject further, other resistances (and conductances) normally expressed in terms of foliar area must be examined.

Mesophyll Resistances, r_m' .

Once pollutant or other gases enter substomatal cavities, they must be either transferred to plant cells, or destroyed by chemical reactions (perhaps involving organic materials generated by the plant itself) within the substomatal cavity or interstices among mesophyll cells. In either case, the practical consequence is that a resistance (per unit foliage area) r_m' , additive to the diffusive stomatal resistance r_s' , is operative (see O'Dell et al., 1977). In classical agrometeorology, mesophyll resistance arises as an important issue in the case of the transfer of carbon dioxide, since CO₂ is relatively insoluble in water. In this context, the arguments of Liss and Slater (1974) regarding the surface conductivity associated with partially soluble chemical species is important. In practice, therefore, we anticipate the need to extend the Liss and Slater mechanisms of uptake by water surfaces to the case of vegetation so that

$$r_m' \sim f(H). \quad (B.6)$$

where H is the Henry's law constant. This constant varies strongly with chemical species. According to Peters (1984), H is 2.19 for ozone and 0.0078 for sulfur dioxide, at 15°C. At this time, however, there is little experimental evidence that would permit discussion of the functional relationship of r_m' and H . Moreover, there is no basis yet for identifying the independent roles of solubility, chemical reactions in the cavity, and reactions occurring on contact with (wet) cellular surfaces in the mesophyll.

Combining Stomatal and Mesophyll Resistances.

Knowledge of r'_s (and to a lesser extent r'_m) has resulted largely from studies of surface heat exchange. There is a considerable body of data from which corresponding values of r'_m and r'_s can be extracted as a function of plant species. Since transfer through stomata is by molecular diffusion, the case of trace gases can be addressed by a simple modification of Equation B.1. In general, r'_s and r'_m are additive. The overall resistance to transfer via the stomata is then

$$r'_{so} = r'_s \cdot Sc \cdot Pr^{-1} + r'_m \quad (B.7)$$

The Prandtl number, $Pr \equiv \nu/\kappa$, enters solely to account for the fact that the Schmidt number Sc is defined in terms of kinematic viscosity, whereas the available knowledge is more applicable to water vapor and heat than momentum.

Cuticular Resistance.

The quantity r'_s represents the effective resistance per unit foliage area associated with transfer of a gas of diffusivity, D , and Henry's law constant, H , via stomata. In practice, a parallel pathway directly to the cuticular surface of foliage is likely to be of equivalent importance for some trace gases, such as fat-soluble hydrocarbons depositing to foliage with waxy leaves. There is little known about how cuticular resistance, r'_{cut} , varies with the chemical characteristics of the material being transferred or with the cuticular characteristics of leaves. At this time, r'_{cut} is introduced for completeness of the analytical model, not because it is a well-known factor.

Extension to Entire Canopy

In general, the net resistance to transfer of gases to a unit area of foliar surface should be written as

$$r'_c = (r'^{-1}_{cut} + r'^{-1}_{so})^{-1} \quad (B.8)$$

As a first attempt to extend relations of this kind to a plant canopy, many workers scale according to leaf area index (LAI). For simple canopies (e.g., crops), such simple scaling is often adequate; however, forests present problems that are targets for current research. Figure B.1 presents an example of the distribution of plant area within a mixed-species forest (after Hutchison et al., 1984). Because stomatal resistance is a strong function of radiation, and because radiation is

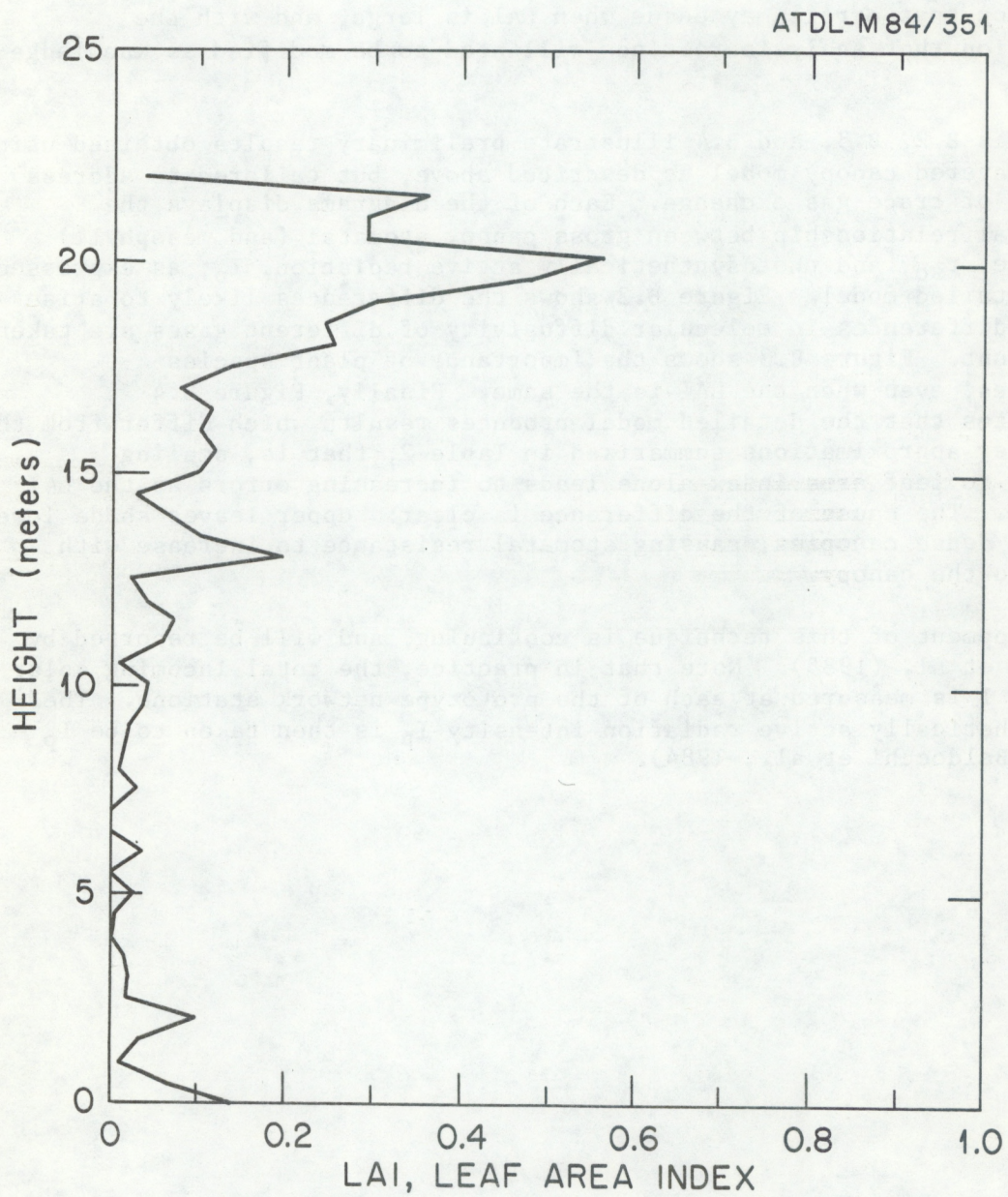


Figure B.1. Vertical distribution of leaf area index for a fully-leaved deciduous forest in summer. The data were obtained at the oak-hickory forest meteorology research site in Oak Ridge, Tennessee.

strongly attenuated and diffused by a canopy, it is clear that a layer-by-layer computation of net overall resistance is especially appropriate for a canopy with large LAI.

The techniques necessary to synthesize overall canopy behavior from knowledge of individual stomatal, mesophyll, and cuticular resistances are discussed by Norman (1980, 1982), who computes canopy conductance from consideration of layers defined to have equal LAI. Appropriate methods are still being developed. Since no definitive results are yet available, first-order scaling according to LAI must be used at this time, with the recognition that errors may ensue when LAI is large, and with the anticipation that analysis routines will need to be modified as knowledge improves.

Figures B.2, B.3, and B.4 illustrate preliminary results obtained using a multi-layered canopy model as described above, but tailored to address questions of trace gas exchange. Each of the diagrams displays the fundamental relationship between gross canopy stomatal (and mesophyll) resistance, r_{so} , and photosynthetically active radiation, I_p , as expressed by the detailed model. Figure B.2 shows the differences likely to arise when the differences in molecular diffusivity of different gases are taken into account. Figure B.3 shows the importance of plant species differences, even when the LAI is the same. Finally, Figure B.4 demonstrates that the detailed model produces results which differ from the first-order approximations summarized in Table 2; that is, scaling according to leaf area index alone leads to increasing errors as the LAI increases. The cause of the difference is clear: upper leaves shade lower leaves in dense canopies, causing stomatal resistance to increase with depth into the canopy.

Development of this technique is continuing, and will be reported by Baldocchi et al. (1985). Note that in practice, the total incoming solar radiation I is measured at each of the prototype network stations. The photosynthetically active radiation intensity I_p is then taken to be $I_p = 0.49 I$, (Baldocchi et al., 1984).

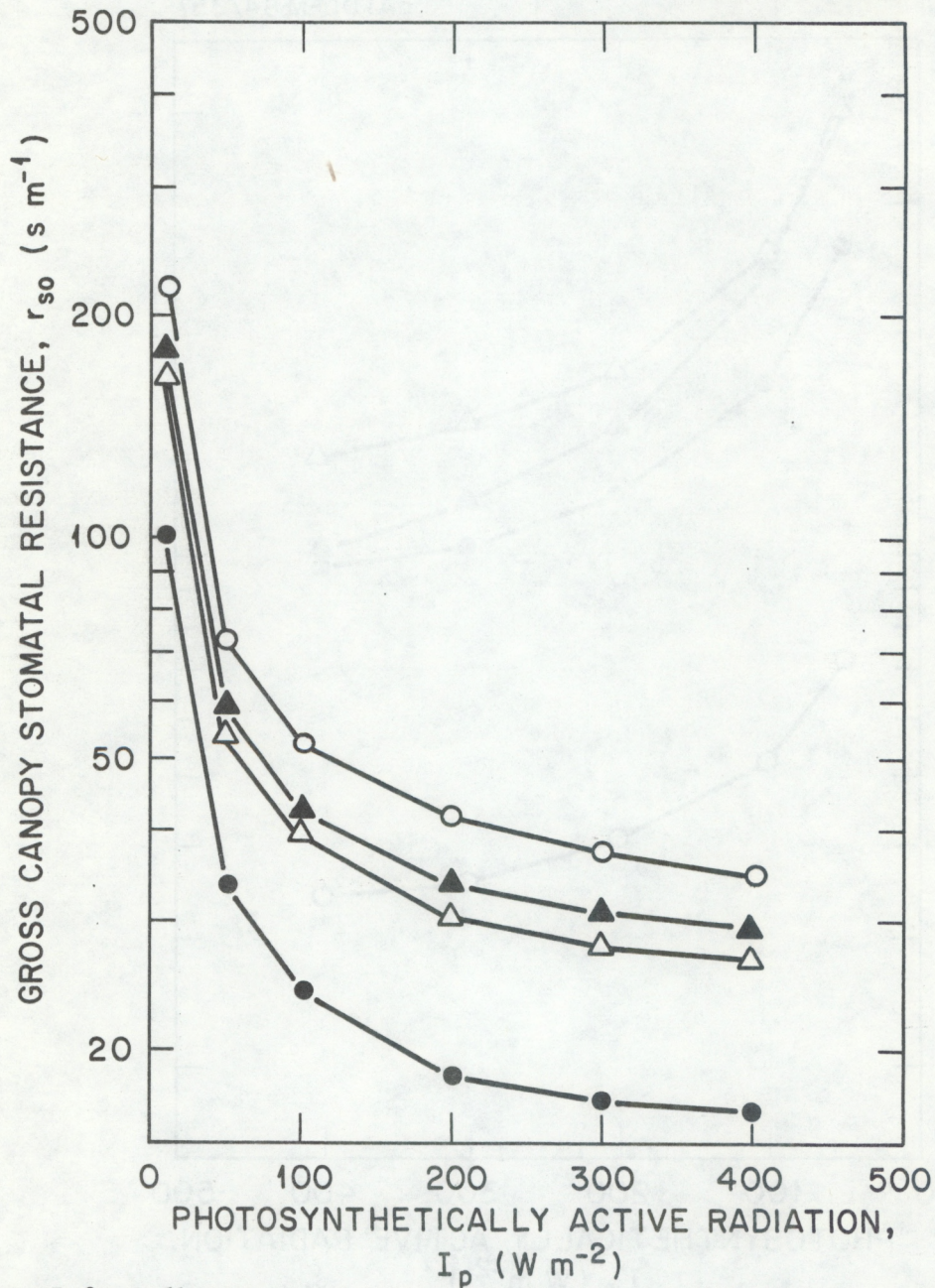


Figure B.2.-Bulk canopy stomatal resistance to water vapor exchange (●), carbon dioxide (Δ), ozone (\blacktriangle), and sulfur dioxide (\circ), computed to demonstrate the dependence on photosynthetically active radiation using a multi-layer model of a soybean canopy (Baldocchi et al., 1985).

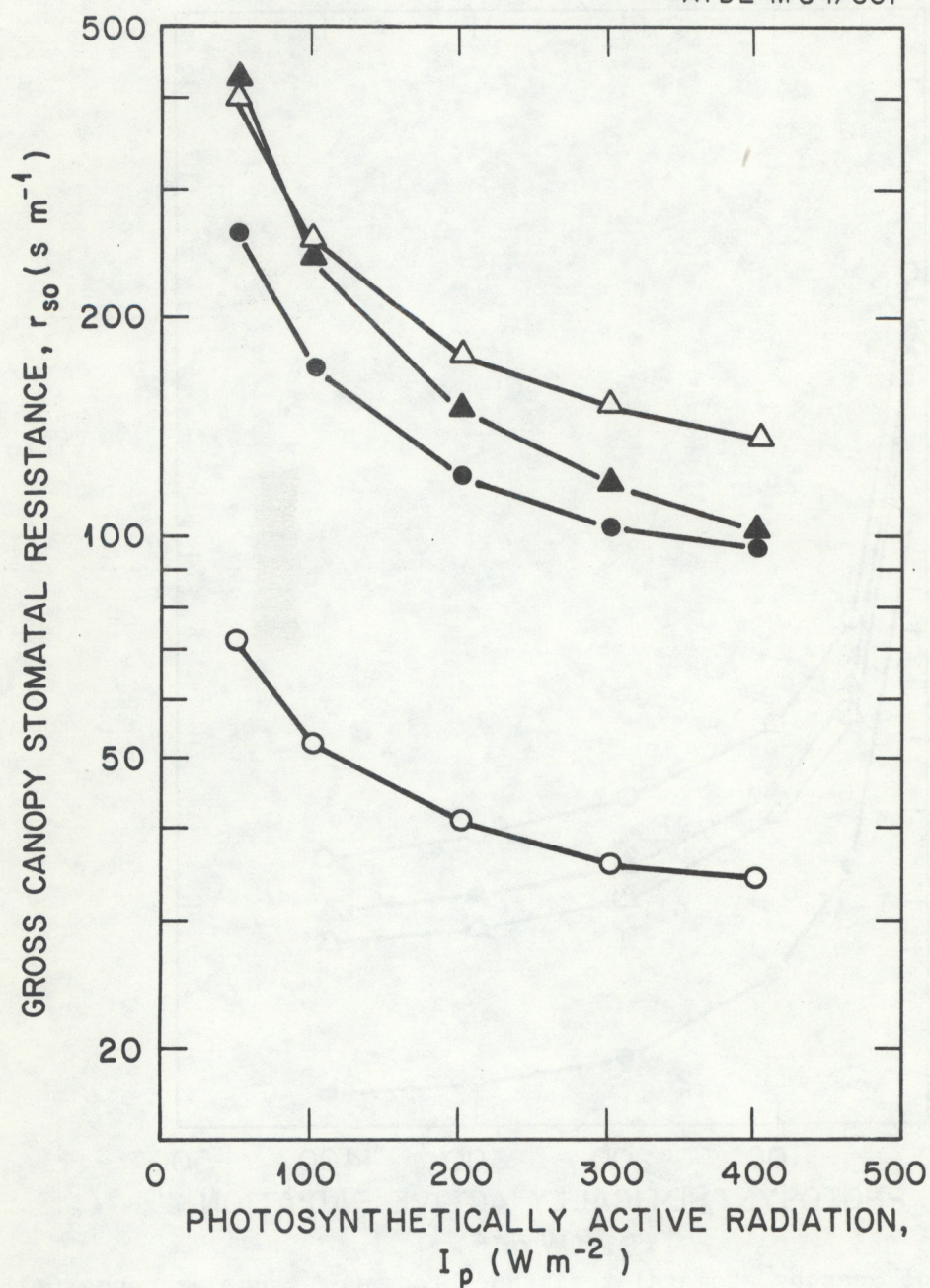


Figure B.3.-Bulk canopy stomatal resistance to sulfur dioxide transfer for four different canopies, oak (●), spruce (Δ), maize (▲), and soybeans (○), derived using the same model as in Figure B.2.

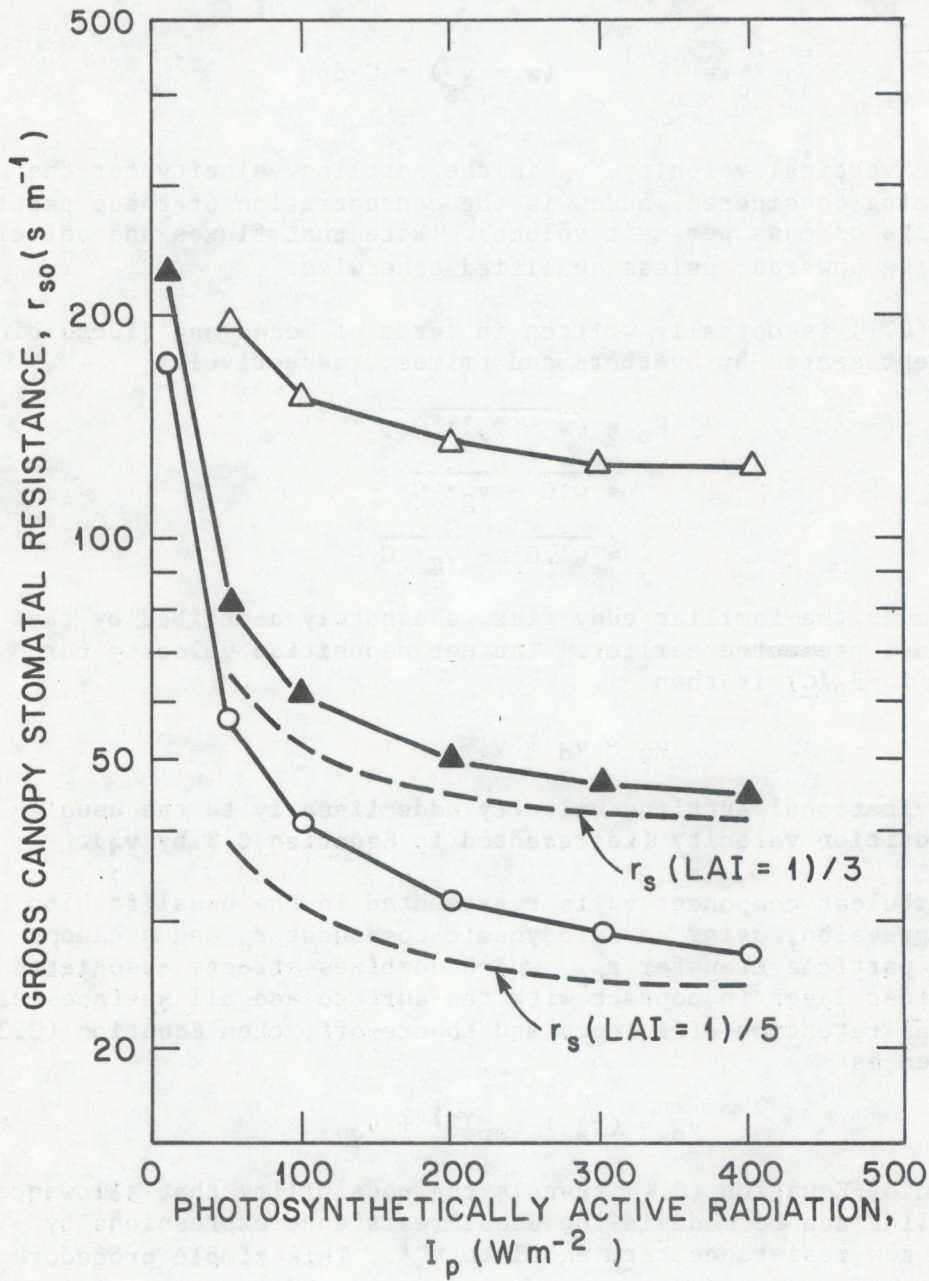


Figure B.4.-The effects of leaf area index on canopy stomatal resistance computed as in Figure B.2, for LAI = 1(Δ), 3(\blacktriangle), and 5(o). Values derived using the simple methods of Table 2 are also shown as dotted lines.

Appendix C: Particle Deposition to Canopies

Background

The fact that particles can fall through the turbulent eddies that transfer trace gases raises questions about how particle transfer can be accommodated within the multiple-resistance framework developed for trace gases. It is informative to consider particle transfer from the viewpoint of turbulent transport. At any point sufficiently above the surface, we can write an expression for the vertical flux of particles F_p as

$$F_p = T^{-1} \int_0^T (w - v_g) \cdot C \, dt \quad (C.1)$$

where w is the vertical velocity, v_g is the settling velocity for the kind of particle being considered, and C is the concentration of these particles in air (in units of mass per unit volume). Note that fluxes and velocities are all positive upwards, unless qualified otherwise.

Equation (C.1) is normally written in terms of means and fluctuating quantities, represented by overbars and primes, respectively:

$$\begin{aligned} F_p &= \overline{(w - v_g) \cdot C} \\ &= \overline{w \cdot C} - \overline{v_g \cdot C} \\ &= \overline{w' \cdot C'} - \overline{v_g \cdot C} \end{aligned} \quad (C.2)$$

The first term is the familiar eddy flux, adequately described by the resistance model presented earlier. The net deposition velocity for particles ($v_p \equiv -F_p/C$) is then

$$v_p = v_d + v_g \quad (C.3)$$

Thus, the gravitational settling velocity adds linearly to the usual turbulent deposition velocity (represented in Equation C.3 by v_d).

If the turbulent component v_d is represented in the usual fashion by a resistance expression, using an aerodynamic component r_a and a canopy resistance to particle transfer r_{cp} , which combines effects associated with the quasi-laminar layer in contact with the surface and all surface-related factors such as retention efficiency and bounce-off, then Equation (C.3) can be expanded as

$$v_p = (r_a + r_{cp})^{-1} + v_g \quad (C.4)$$

Inspection of Equation (C.4) reveals the possibility that allowance for particle settling can be made in the usual resistance expressions by introducing a new resistance term equal to v_g^{-1} . This simple procedure introduces a conceptual problem, however, since obviously both v_d and C are functions of height and v_g is not. The questions that arise can better be addressed as follows:

$$F_p = - [C(z) - C(z_0)] \cdot r_a^{-1} - C(z) \cdot v_g \quad (C.5)$$

where z_0 is the appropriate roughness length. (Note that F_p is positive upwards.) At height z_0 , we can write a separate relation for the same flux (assumed constant with height)

$$F_p = - C(z_0) \cdot r_{cp}^{-1} - C(z_0) \cdot v_g \quad (C.6)$$

After eliminating the intermediate concentration $C(z_0)$ from Equation (C.5) and Equation (C.6), algebraic manipulation yields

$$v_p = v_g + (r_a + r_{cp} + r_a r_{cp} v_g)^{-1} \quad (C.7)$$

This relation differs from the usual form by inclusion of a term involving gravitational settling within the resistance expansion. Figure C.1 shows how the familiar resistance model can be modified in order to reproduce the behavior predicted by the mathematics given above.

In practice, the triple-product term in Equation (C.7) is unlikely to be of great significance unless v_g is relatively large. Detailed consideration of the ramifications is not warranted, since great uncertainty surrounds the quantity r_{cp} for the case of particles.

Estimating Particle Deposition

It is well known that particle size has a dominating influence on the deposition velocity that should be applied to air concentrations in order to evaluate dry deposition. This knowledge comes from modeling studies, both physical and theoretical, of deposition to simple uniform surfaces. Experimental techniques for measuring particle deposition to natural surfaces are still in their infancy. At this stage, it is probably not warranted to examine the various (and often contradictory) experimental and theoretical evidence in detail (see discussion elsewhere, e.g., Hicks, 1984).

In fact, the wide variety of models intended to describe particle deposition to vegetated canopies is evidence of the poor state of contemporary knowledge. These models range in complexity from very simple descriptions of experimental data to relatively complicated schemes describing turbulent transfer inside canopies and the impaction and interception of particles. It must be remembered that we cannot yet agree on how best to simulate atmosphere-canopy interaction for heat and momentum, let alone trace gases (including H_2O) and aerosols. Moreover, we must be careful not to confuse data and models referring to individual surface elements of the canopy with results appropriate for the canopy as a whole. In the present context, the emphasis is necessarily on the characteristics of an entire canopy, not on where deposition occurs within the canopy.

The case of deposition to grass-like surfaces with leaf area indices near unity is less uncertain. In practice, the outstanding difficulty confronting contemporary research on particle deposition is how to

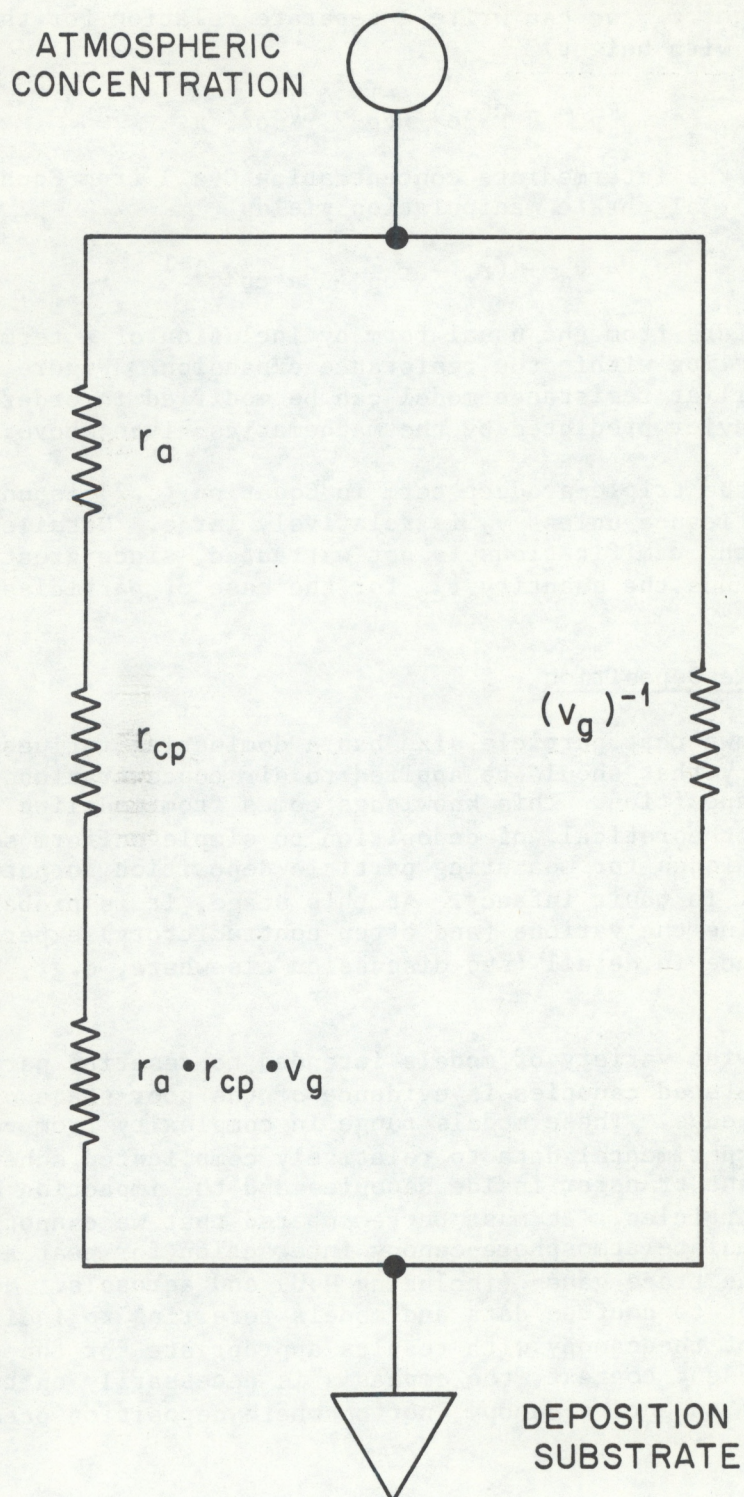


Figure C.1.-The conceptual resistance model associated with the transfer of particles. The term $r_a \cdot r_s \cdot v_g$ is included to satisfy the formalism of Equation C.7.

synthesize the behavior of a forest canopy from first principles, usually starting from knowledge of characteristics of particle deposition on flat plates and pipes.

Belot et al. (1976), Bache (1979), Davidson et al. (1982), Slinn (1982), and de la Mara and Friedlander (1982) present examples of models designed to extend laboratory data on deposition to surrogate surfaces to real-world plant canopies. These models vary widely in their assumptions and in their predictions. However, all predict deposition velocities substantially lower than observed in experiments involving deposition of naturally occurring radionuclides to plant surfaces (Russell et al., 1981; $v_d \sim 0.03\text{--}0.05$ cm/s for submicron aerosol deposition to individual plant surfaces, hence perhaps 0.3 to 0.5 cm/s to the canopy as a whole), leaf washing (Lindberg et al., 1983; $v_d \approx 0.4$ cm/s for sulfate to deciduous forest), and micrometeorology (Hicks et al., 1982; $v_d \approx 0.7$ cm/s for daytime deposition of sulfate aerosol to a pine forest).

The state of knowledge regarding particle deposition to vegetative canopies is presently so poor that no "best" model can yet be identified. As an interim measure, therefore, a purely empirical relationship appears equally acceptable. Figure C.2 after Wesely et al. (1983), shows an approximately linear relationship between v_d for small particles and the product $\sigma_\theta u$:

$$v_d \approx 0.003 \sigma_\theta \bar{u}. \quad (\text{C.8})$$

It is not yet clear how Equation (C.8) can best be integrated with the formalism developed earlier, mainly for trace gases. However, it is obvious that a dependence on Schmidt number Sc is required. Wesely et al. (1983) emphasize the uncertainties involved in any assumption regarding the role of Sc . They point out that Brutsaert (1979) recommends a Schmidt number exponent of about 0.5 for use in fully-rough flow such as over forests. In comparison, Hicks (1984) continues to advocate exponents near 2/3. For small particles, the difference is likely to be very important and could help explain why models do not agree well with field data.

For testing purposes in the monitoring program described here, two independent values of small-particle deposition velocity will be used. The first is derived directly as an extension of the canopy model described in Appendix B, taking into account such factors as the irrelevance of the stomatal resistance and the need to consider double-sided leaf area indices rather than single-sided. The second is purely empirical, as indicated in Figure C.2. Both are intended to yield results appropriate to the particulate species associated with the entire spectrum of accumulation-size-range aerosols. A target of the research programs that are concurrent with this exploratory effort must be to resolve the differences that arise. At this time, however, it is not known how important these differences are.

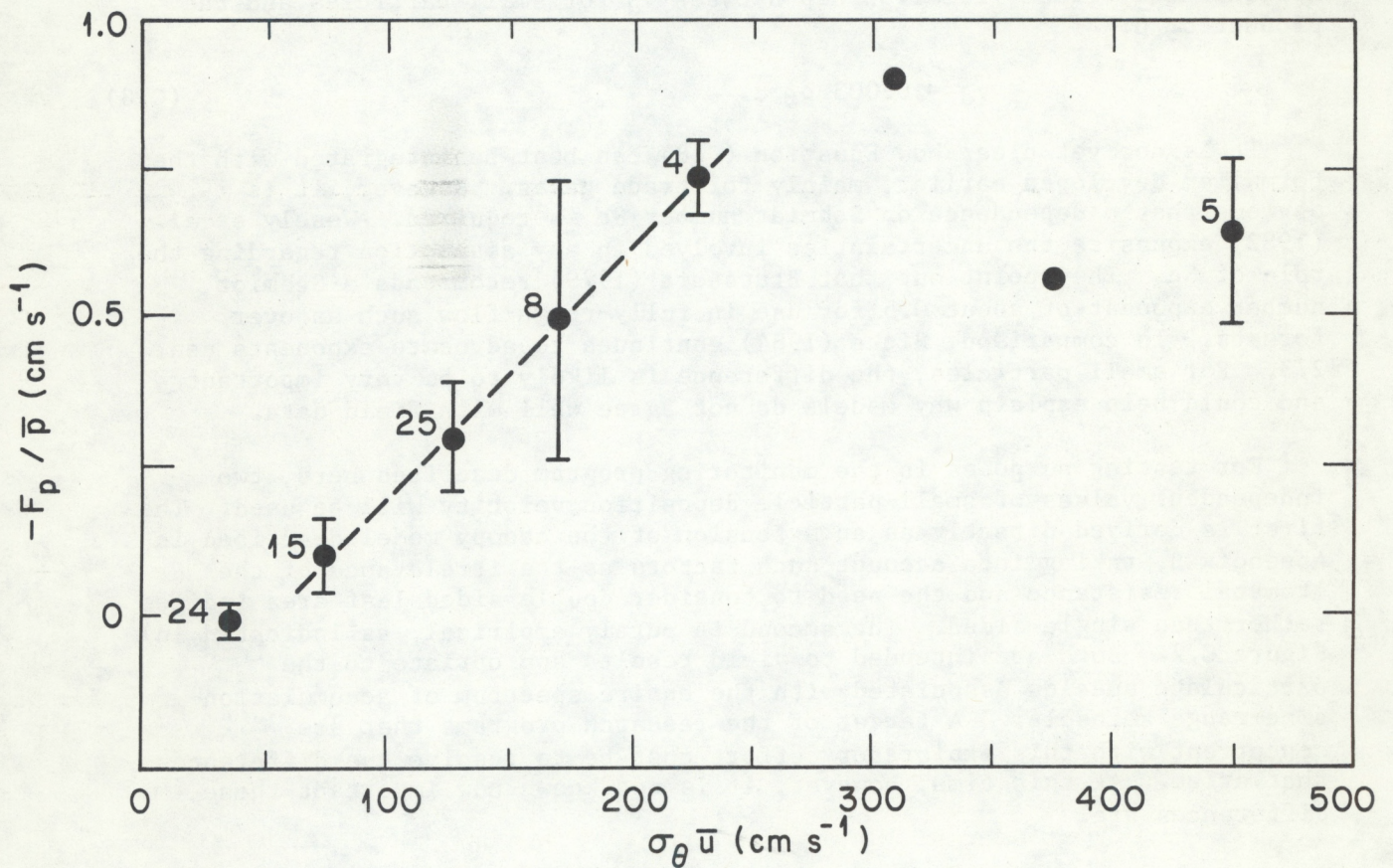


Figure C.2.-Fine-particle deposition velocity as a function of $\sigma_{\theta} \cdot u$, with standard error and the number of contributing measurements indicated. Values were obtained over a deciduous forest in winter, with no snow present (see Wesely et al., 1983).

Appendix D: Program Listing and Explanation

Discussion

The program presently used to compute deposition velocities from routinely collected meteorological data is listed in Section 2. This program takes as input the quantities identified in the main text of this document, with supporting data provided by site operators, based on visual observations made weekly.

Data recorded at individual sites are first examined in order to detect (and reject) errors, and to interpolate through short periods of missing data. On-site checks and data tests are performed to ensure that sensors and recording apparatus are working correctly. The programs used in this data quality assurance work are given elsewhere (Hosker *et al.*, 1985). After completion of such tests, values of the separate resistances r_a , r_b , and r_c are computed.

Aerodynamic resistance is evaluated from the measured wind speeds and from measurements of the standard deviation of wind direction. The method (as described in Section 5) minimizes the need to evaluate the effects of atmospheric stability; observed values of σ_θ are used to incorporate such effects in the computation. Aerodynamic resistance is not influenced by the species of pollutant under consideration.

Quasi-laminar boundary layer resistance r_b is derived from the same wind data, but with an accounting for effects of molecular or Brownian diffusivity of the trace gas or particulate species under consideration.

Canopy resistance r_c is computed from site-specific biological information regarding the kind of vegetation, its present leaf area index, and its current biological state. Canopy wetness is estimated using artificial wetness sensors as surrogates. While these devices cannot be expected to provide a precise measure of the wetness of the canopy itself, they certainly provide an indication of surface wetness that is superior to the alternative assumption that the foliage is never wet. Insolation is measured directly, yielding estimates of photosynthetically active radiation, from which stomatal resistance is evaluated. Temperature and humidity data lead to correction factors that are applied to stomatal resistance estimates.

All of the procedures used in this analysis are under continuing review, involving both the improvement of relevant theories and simulations and direct comparison with more detailed and sophisticated experimental observations made at specially-selected sites.

The analytical routine listed here is viewed as a slowly-improving facility to interpret meteorological and surface data, and is as yet far from the point at which general application can be suggested. Figures D.1, D.2, D.3, and D.4 show a typical sequence of outputs of the routine, for the first four weeks of 1985. The data shown are for the Oak Ridge site. Some features of the data are worthy of special note.

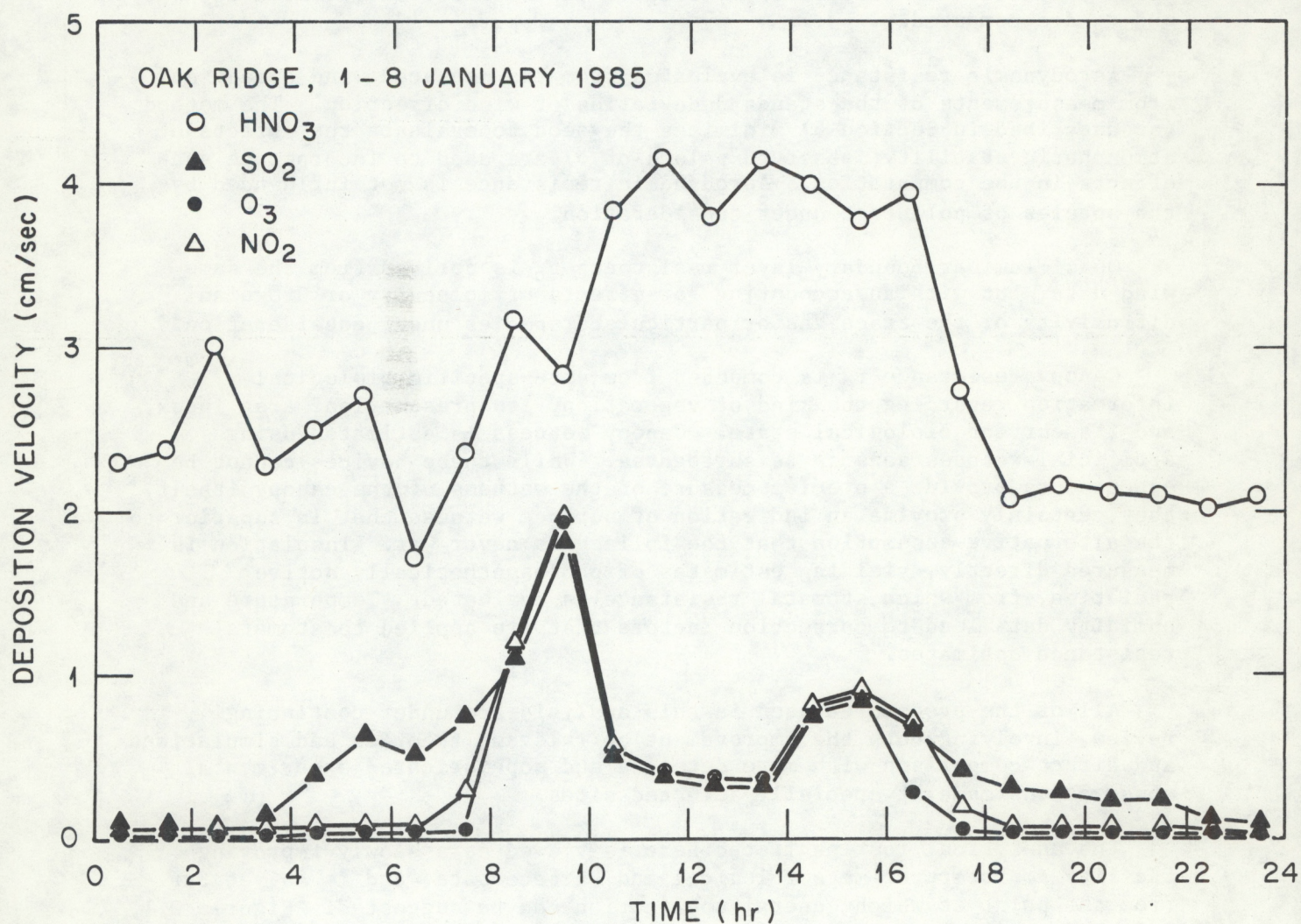


Figure D.1.-The weekly-average diurnal cycle of deposition velocity for HNO_3 , SO_2 , O_3 , and NO_2 , deduced for the Oak Ridge site using the methods described here, for the first week of 1985.

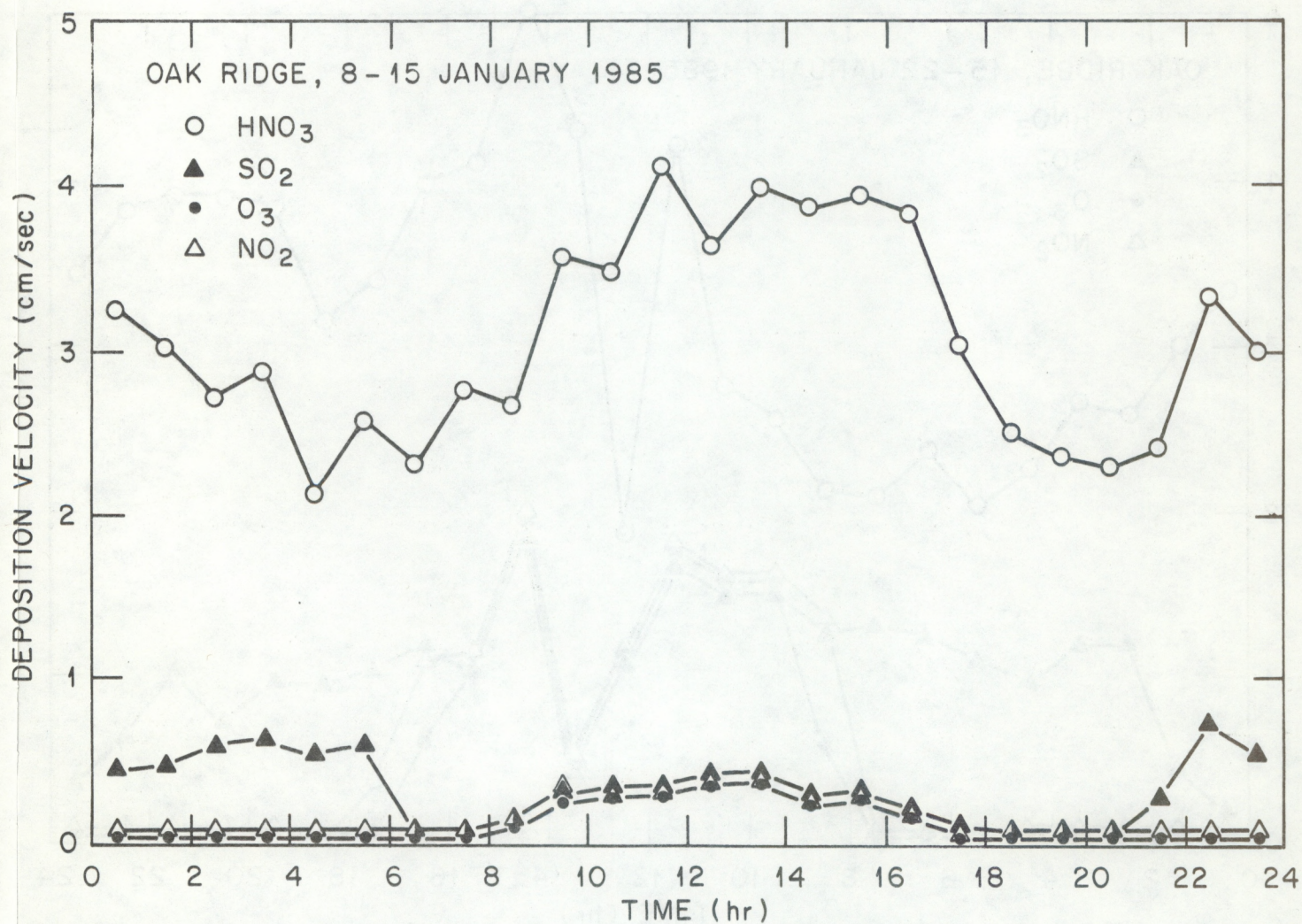


Figure D.2.-The weekly-average diurnal cycle of deposition velocity for HNO_3 , SO_2 , O_3 , and NO_2 , deduced for the Oak Ridge site using the methods described here, for the second week of 1985.

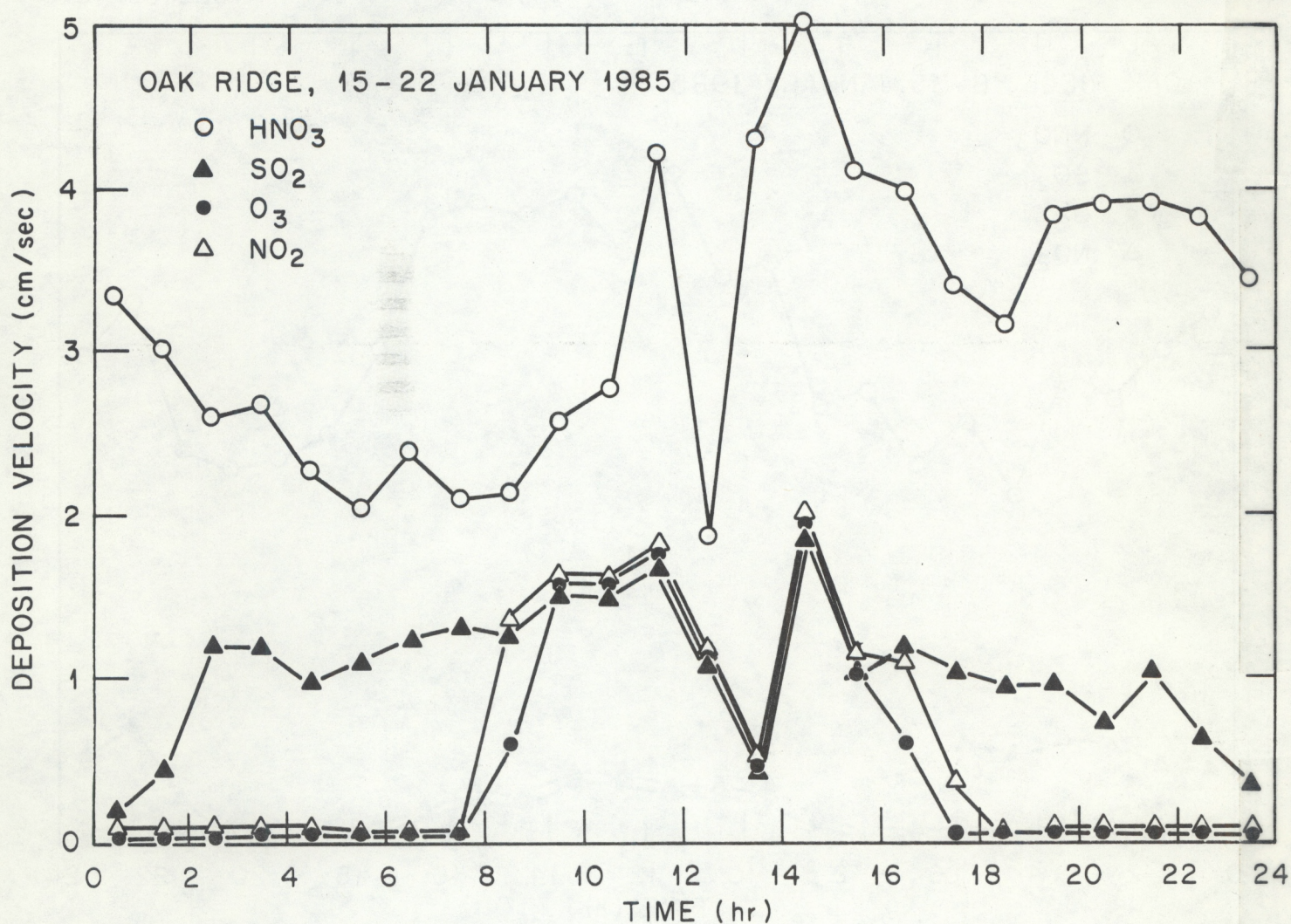


Figure D.3.-The weekly-average diurnal cycle of deposition velocity for HNO_3 , SO_2 , O_3 , and NO_2 , deduced for the Oak Ridge site using the methods described here, for the third week of 1985.

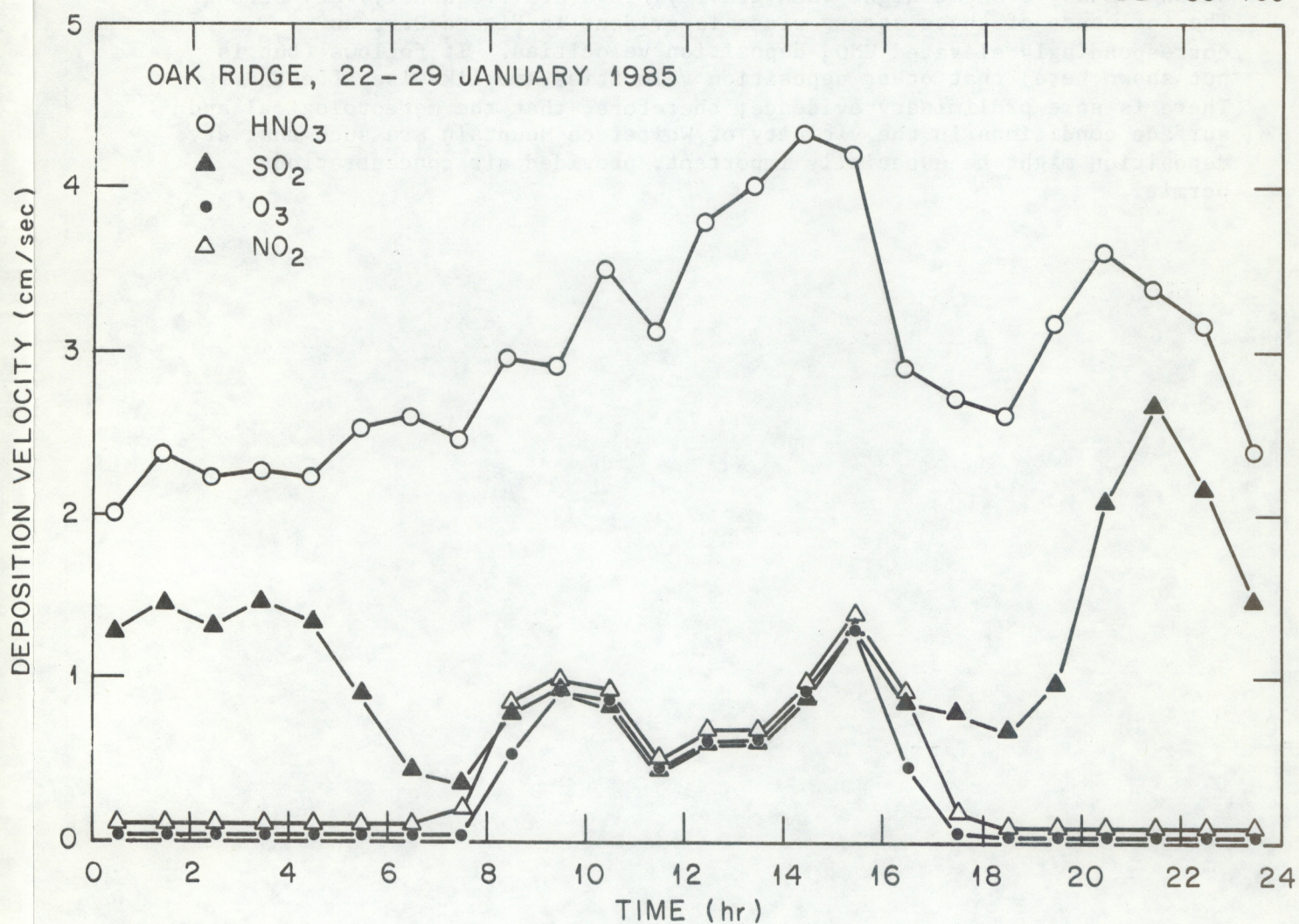


Figure D.4.-The weekly-average diurnal cycle of deposition velocity for HNO_3 , SO_2 , O_3 , and NO_2 , deduced for the Oak Ridge site using the methods described here, for the fourth week of 1985.

- (i) The diurnal cycle is clearly evident for most species considered, but the reduction to near-zero at night is only typical for O_3 and NO_2 .
- (ii) Effects of surface moisture can sometimes be seen in the SO_2 behavior, with considerably elevated deposition velocities at night when the surface is wet.
- (iii) Week-to-week variability is considerable.

The matter of site variability is illustrated in Figure D.5. Here, it is seen that for HNO_3 , similar behavior is expected at all of the locations presently being used to test the methods advocated here, with the exception of Whiteface Mountain. The Whiteface Mountain site is located on the slope of the mountain, about half-way to the summit. It experiences extremely strong winds, even at night when gravity-flows are frequently very strong. The influence of these strong winds is evident in Figure D.5, as correspondingly elevated HNO_3 deposition velocities. It follows (but is not shown here) that other deposition velocities are likewise affected. There is some preliminary evidence, therefore, that the meteorological and surface conditions in the vicinity of Whiteface Mountain are such that dry deposition might be especially important, provided air concentrations permit.

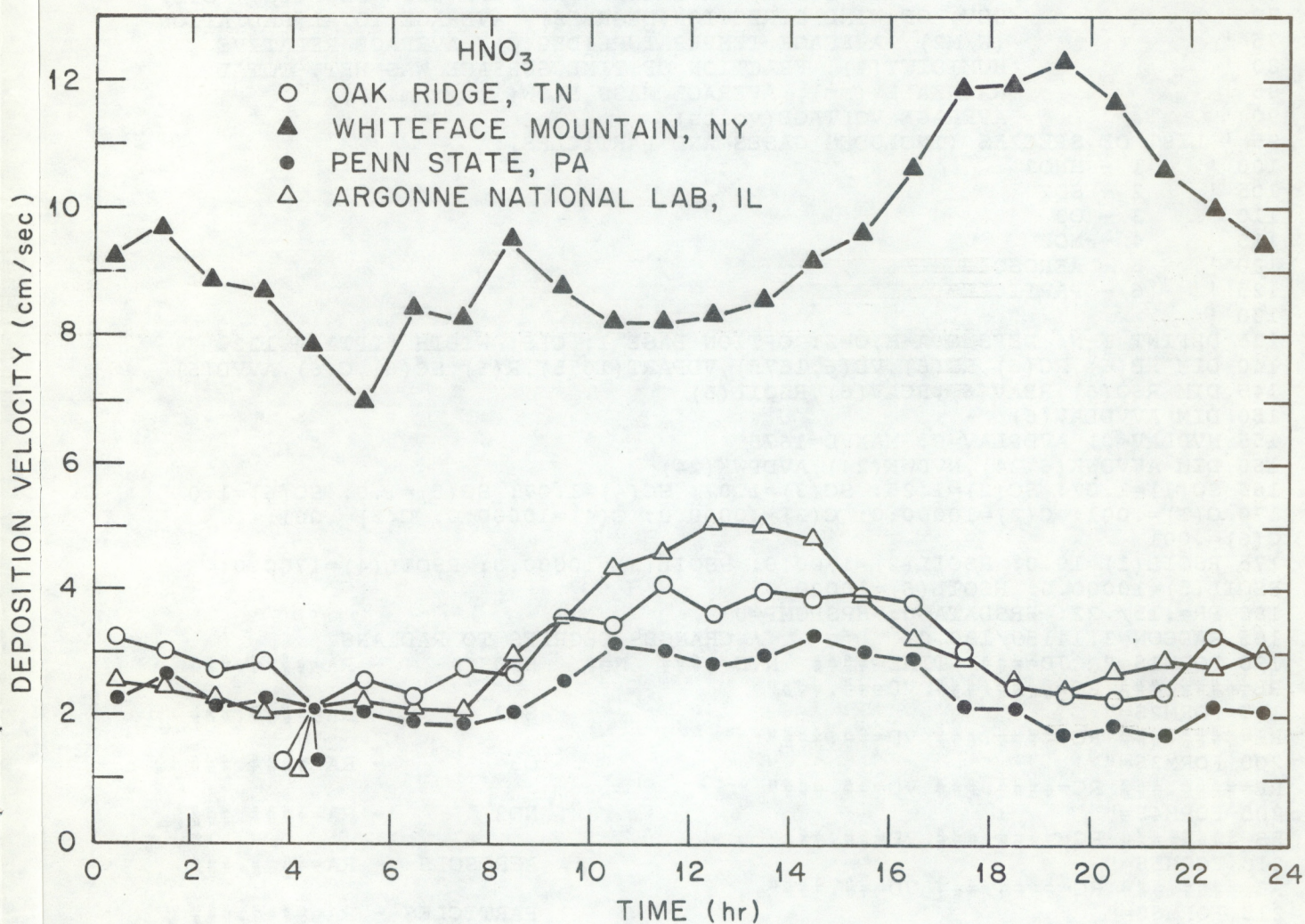


Figure D.5.-Weekly-averaged diurnal cycles of deposition velocity for HNO_3 , as deduced from the routines described here, for locations near Oak Ridge (TN), West Point (NY), State College (PA), and Whiteface Mountain (NY). Data are for the first week of 1985.

Program Listing
As of September 5, 1985

```

5 LPRINT "DEPOSITION VELOCITY MODEL - VERSION 85248": LPRINT: LPRINT
10 'DATA FROM METEOROLOGY -- 15 MINUTE AVERAGES AND HOUR AVERAGES
15 '    15 MINUTE - JULIAN DAY, TIME, TEST VOLTAGE(%), STD. DEV. OF TEST
20 '                VOLTAGE(%), MAXIMUM WIND GUST(m/s), TIME OF MAX WIND
GUST,
25 '                STD. DEV. OF WIND SPEED(m/s), AVERAGE WIND SPEED(m/s),
30 '                AVERAGE WIND VECTOR SPEED(m/s), AVERAGE WIND DIRECTION
35 '                (DEGREES), STD. DEV. OF WIND DIRECTION(DEGREES), AVERAGE
40 '                TOTAL RADIATION(W/M2), AVERAGE TEMPERATURE(DEG.C),
AVERAGE
45 '                RELATIVE HUMIDITY(%), FRACTION OF TIME SURFACE WAS WET,
50 '                TOTAL RAINFALL (mm), AVERAGE MASS FLOW(liter/min),
55 '                STD. DEV. OF MASS FLOW(liter/min), AVERAGE VOLTAGE(volts)
60 '    HOUR - STATION ID NUMBER, AVERAGE WIND SPEED(m/s), AVERAGE WIND
65 '                VECTOR SPEED(m/s), AVERAGE WIND DIRECTION(DEGREES), STD.
70 '                DEV. OF WIND DIRECTION(DEGREES), AVERAGE TOTAL RADIATION
75 '                (W/M2), AVERAGE TEMPERATURE(DEG.C), AVERAGE RELATIVE
80 '                HUMIDITY(%), FRACTION OF TIME SURFACE WAS WET, TOTAL
85 '                RAINFALL (mm), AVERAGE MASS FLOW(liter/min),
90 '                AVERAGE VOLTAGE(volts)
95 ' LIST OF SPECIES (INCLUDES GASES AND PARTICLES):
100 '     1 - HNO3
105 '     2 - SO2
110 '     3 - O3
115 '     4 - NO2
120 '     5 - AEROSOLS
125 '     6 - PARTICLES
130 '
135 DEFINT I-N: DEFSNG A-H,O-Z: OPTION BASE 1: CLS: WIDTH "LPT1:",132
140 DIM RB(6),RC(6),RS(6),VD(6,1675),VDPART(1675),R(6),SC(6),C(6),AVVD(6)
145 DIM RSO(6),RBAV(6),RCAV(6),RSOIL(6)
150 DIM AVVDLAV(6)
155 NVDLAV=0: AVDPLAV=0: MAXVD=1675
160 DIM AVVDWK(6,24),NVDWK(24),AVDPWK(24)
165 SC(1)=1.07: SC(2)=1.25: SC(3)=1.07: SC(4)=1.07: SC(5)=1.0: SC(6)=1.0
170 C(1)=.001: C(2)=10000.0: C(3)=10000.0: C(4)=10000.0: C(5)=.001:
C(6)=.001
175 RSOIL(1)=10.0: RSOIL(2)=1700.0: RSOIL(3)=10000.0: RSOIL(4)=1700.0:
RSOIL(5)=10000.0: RSOIL(6)=10000.0
180 PR=.15/.22: HRSDATA=0: HRSPUMP=0
185 RADCON=3.14159/180.0 ' CHANGES DEGREES TO RADIANS
190 FORM1$=" JD=### TIME=#### NVD=#### N=# HNO3 - RA=####.###
RB=####.### RC=####.### VD=####.###"
195 FORM2$=" SO2 - RA=####.###
RB=####.### RC=####.### VD=####.###"
200 FORM3$=" O3 - RA=####.###
RB=####.### RC=####.### VD=####.###"
205 FORM4$=" NO2 - RA=####.###
RB=####.### RC=####.### VD=####.###"
210 FORM5$=" AEROSOLS - RA=####.###
RB=####.### RC=####.### VD=####.###"
215 FORM6$=" PARTICLES - RA=####.###
RB=####.### RC=####.### VD=####.###,VD=####.###"
220 FORMW1$=" TIME=#### N=#### HNO3 - VD=####.###"
225 FORMW2$=" SO2 - VD=####.###"
230 FORMW3$=" O3 - VD=####.###"
235 FORMW4$=" NO2 - VD=####.###"
240 FORMW5$=" AEROSOLS - VD=####.###"

```



```

515 IF QAV$="W" THEN LPRINT "VD'S AVERAGED BY HOURS OVER WEEK"
520 IF QAV$="L" THEN LPRINT "VD'S AVERAGED OVER HOURS OVER WEEK"
525 IF LOPT=1 THEN LPRINT "LEAFED CANOPY CONSIDERED": LPRINT
530 IF LOPT=2 THEN LPRINT "LEAFLESS CANOPY CONSIDERED": LPRINT
535 '
540 '
545 OPEN DFN$ FOR INPUT AS #1
550 NVD=0: NHR=IHBEG
555 IF NVD=0 THEN GOTO 590
560 IF EOF(1)<>0 THEN GOTO 1205
565 INPUT
#1,NT,ISTID,VAVWS,VAVVS,VAVWD,VSDWD,VAVTR,VAVAT,VAVRH,VTWET,VAVRR,VAVMF,VAV
VOLT
570 IF VAVMF>=2.8 AND VAVMF<=3.2 THEN HRSPUMP=HRSPUMP+1
575 HRSDATA=HRSDATA+1
580 IF EOF(1)<>0 THEN GOTO 1205
585 NHR=1
590 FOR K=NHR TO 4
595 INPUT
#1,NT,JD,IHRMIN,TESTVOLT,SDTVOLT,VMWG,TIMWG,VSDWS,VAVWS,VAVVS,VAVWD,VSDWD,V
AVTR,VAVAT,VAVRH,VTWET
600 IF QAQC$="N" THEN INPUT #1,NT,VAVRR,VAVMF,VSDMF,VAVVOLT
605 IF QAQC$="Y" THEN INPUT #1,NT,IDAYR,VAVRR,VAVMF,VSDMF,VAVVOLT
610 YRJD$=STR$(JD): JULDAY$=RIGHT$(YRJD$,3): JD=VAL(JULDAY$)
615 IF NVD<>0 THEN GOTO 625
620 LPRINT "DATA STARTS --> JULIAN DAY ";JD;" AT ";IHRMIN: LPRINT
625 NVD=NVD+1
630 U=VAVWS: IF U>90.0 OR U<.3 THEN GOTO 990
635 SIGTH=VSDWD: IF SIGTH=0.0 THEN SIGTH=.0001 ELSE IF SIGTH>90.0 THEN GOTO
990
640 RI=VAVTR: IF RI>9000 THEN GOTO 990 ELSE IF RI<1.0 THEN RI=1.0
645 IF VAVAT>90.0 THEN GOTO 990
650 IF VAVAT<0.0 THEN VAVAT=0.0
655 IF VAVAT>40.0 THEN VAVAT=40.0
660 IF VAVAT>=0.0 AND VAVAT<=40.0 THEN NTEMP=CINT(VAVAT) ' CONVERT TEMP TO
INTEGER
665 CWET=0
670 IF VTWET>0.0 AND VTWET<=1.0 THEN CWET=1
675 IF VAVRR>0.0 AND VAVRR<200.0 THEN CWET=1
680 IF QAV$="H" THEN LPRINT U,SIGTH,RI,NTEMP,CWET
685 IF QAV$="W" THEN PRINT JD,IHRMIN,NT
690 RIP=.49*RI
695 SIGTH=SIGTH*RADCON
700 ' RI=AVERAGE SOLAR RADIATION (W/m2)
705 ' U=AVERAGE WIND SPEED (m/sec)
710 ' SIGTH=STANDARD DEVIATION OF WIND DIRECTION (radians)
715 ' NTEMP=TEMPERATURE IN INTEGER FORM (deg C)
720 ' CWET=0 IF CANOPY NOT WET, 1 IF IT IS
725 ' RIP=PHOTOSYNTHETICALLY ACTIVE RADIATION (W/m2)
730 ' RRS=BASIC STOMATAL CONDUCTANCE (sec/m)
735 ' FE=VAPOR PRESSURE DEFICIT CORRECTION
740 ' FW=WATER STRESS CORRECTION FACTOR
745 ' FT=THERMAL STRESS CORRECTION FACTOR
750 ' RRM=MESOPHYLL RESISTANCE (sec/m)
755 ' RSO=OVERALL RESISTANCE VIA STOMATA (sec/m)
760 ' RC=RESISTANCE FOR CANOPY (sec/m)
765 ' RA=AERODYNAMIC RESISTANCE (sec/m)
770 ' RB=QUASI-LAMINAR BOUNDARY RESISTANCE (sec/m)
775 ' R=TOTAL RESISTANCE (sec/m)
780 ' VD=DRY DEPOSITION VELOCITY (cm/sec)
785 ' RSM=MINIMUM STOMATAL RESISTANCE (sec/m)

```



```

790 ' B=COEFFICIENT CONTROLLING STOMATAL CONDUCTANCE (sec m/W)
795 ' C=LIMITING CUTICULAR RESISTANCE (sec/m)
800 ' RLAI=LEAF AREA INDEX
805 ' RSOIL=SOIL RESISTANCE (sec/m)
810 VDPART(NVD)=.003*SIGTH*U
815 VDPART(NVD)=VDPART(NVD)*100.0 ' CONVERT FROM m/sec TO cm/sec
820 FOR I=1 TO NSPEC
825 RRS=(1.0/RSM)*(1.0/(1.0+B/RIP))
830 FE=1.0
835 FW=1.0
840 FT=1.0
845 RRS=1.0/(RRS*FE*FW*FT)
850 RRS=RRS*SC(I)/PR
855 RRM=0.0
860 RSO(I)=RRS+RRM: IF RSO(I)=0.0 THEN RSO(I)=.001
865 ' ACCOUNT FOR CUTICULAR RESISTANCE AND LEAF AREA INDEX
870 RC(I)=((RSO(I)^-1)+(C(I)^-1))^-1/RLAI
875 ' ACCOUNT FOR SOIL RESISTANCE
880 IF I<>5 THEN RC(I)=((RC(I)^-1)+(RSOIL(I)^-1))^-1 ELSE
RC(I)=(U*SIGTH)*100
885 IF CWET=0 THEN GOTO 925 ' CONSIDER CANOPY WETNESS WHEN DETERMINING RC
890 ' IF WETNESS DETECTED, THEN LIMIT SPECIES 1-4
895 ON I GOTO 910,910,900,900,915,915,915,915,915
900 IF RC(I)>1000 THEN RC(I)=1000
905 GOTO 915
910 IF RC(I)>.2 THEN RC(I)=.2
915 ' FOR AEROSOLS, USE DOUBLE-SIDED LAI
920 IF I=5 THEN RC(I)=RC(I)/2.0
925 NEXT I
930 RADN=U*SIGTH*SIGTH
935 IF SIGTH>.175 AND RI>100.0 THEN RA=9.0/RADN ELSE RA=4.0/RADN ' A=10
DEGREES
940 IF U<.3 AND RI<100.0 THEN RA=1500.0
945 IF U<.3 AND RI>=100.0 THEN RA=10.0
950 USTAR=(U/RA)^.5
955 FOR I=1 TO NSPEC
960 RB(I)=2.0*(1.0/(.4*USTAR))
965 RB(I)=RB(I)*(SC(I)/PR)^(2.0/3.0)
970 R(I)=RA+RB(I)+RC(I)
975 VD(I,NVD)=100.0/R(I)
980 NEXT I
985 ' OUTPUT VD RESULTS
986 IF DFOUT$="" THEN GOTO 990
987 PRINT #3, USING FORMOUT$;
JD;IHRMIN;VD(1,NVD);VD(2,NVD);VD(3,NVD);VD(4,NVD);VD(5,NVD);VD(6,NVD);VDPAR
T(NVD)
990 MINUT$=STR$(IHRMIN): MIN$=RIGHT$(MINUT$,2): MINIT=VAL(MIN$)
995 IHRNDX=(IHRMIN-MINIT)/100+1: IF MINIT=0 THEN IHRNDX=IHRNDX-1
1000 PRINT JD,IHRMIN,MINIT,IHRNDX
1005 IF QAV$="H" THEN GOTO 1010 ELSE GOTO 1150
1010 ' AVERAGE TOGETHER TIMES ENDING WITH 15,30,45,0 TO GET HOUR AVERAGES
1015 IF NVD>1 THEN GOTO 1035
1020 FOR L=1 TO NSPEC
1025 AVVD(L)=0.0: RBAV(L)=0.0: RCAV(L)=0.0
1030 NEXT L: N=0: AVVDP=0.0: RAAV=0.0
1035 IFLAG=0
1040 IF MINIT<>0 THEN GOTO 1050
1045 IFLAG=1
1050 IF MINIT=30 THEN ITIME=IHRMIN ELSE ITIME=((IHRMIN/100)-1)*100+30
1055 IF VD(1,NVD)<0 THEN GOTO 1070

```



```

1060 FOR L=1 TO NSPEC: AVVD(L)=AVVD(L)+VD(L,NVD): RBAV(L)=RBAV(L)+RB(L):
RCAV(L)=RCAV(L)+RC(L): NEXT L
1065 AVVDP=AVVDP+VDPART(NVD): RAAV=RAAV+RA: N=N+1
1070 IF IFLAG=0 THEN GOTO 1190
1075 IF N=0 THEN GOTO 1190
1080 FOR L=1 TO NSPEC: AVVD(L)=AVVD(L)/N: RBAV(L)=RBAV(L)/N:
RCAV(L)=RCAV(L)/N: NEXT L
1085 AVVDP=AVVDP/N: RAAV=RAAV/N
1090 LPRINT USING FORM1$;JD,ITIME,NVD,N,RAAV,RBAV(1),RCAV(1),AVVD(1)
1095 LPRINT USING FORM2$;RAAV,RBAV(2),RCAV(2),AVVD(2)
1100 LPRINT USING FORM3$;RAAV,RBAV(3),RCAV(3),AVVD(3)
1105 LPRINT USING FORM4$;RAAV,RBAV(4),RCAV(4),AVVD(4)
1110 LPRINT USING FORM5$;RAAV,RBAV(5),RCAV(5),AVVD(5)
1115 LPRINT USING FORM6$;RAAV,RBAV(6),RCAV(6),AVVD(6),AVVDP
1120 LPRINT
1135 FOR L=1 TO NSPEC: AVVD(L)=0.0: RBAV(L)=0.0: RCAV(L)=0.0: NEXT L
1140 N=0: AVVDP=0.0: RAAV=0.0
1145 GOTO 1190
1150 ' AVERAGE TOGETHER TIMES TO GET WEEKLY AVERAGE (24 TABLES)
1155 IF NVD>1 THEN GOTO 1175
1160 FOR M=1 TO 24
1165 FOR L=1 TO NSPEC: AVVDWK(L,M)=0.0: NEXT L
1170 NVDWK(M)=0: AVDPWK(M)=0.0: NEXT M
1175 IF VD(1,NVD)<0.0 THEN GOTO 1190
1180 FOR L=1 TO NSPEC: AVVDWK(L,IHRNDX)=AVVDWK(L,IHRNDX)+VD(L,NVD): NEXT L
1185 NVDWK(IHRNDX)=NVDWK(IHRNDX)+1:
AVDPWK(IHRNDX)=AVDPWK(IHRNDX)+VDPART(NVD)
1190 IF EOF(1)<>0 THEN GOTO 1205
1195 NEXT K
1200 GOTO 560
1205 CLOSE #1: LPRINT "DATA ENDS --> JULIAN DAY ";JD;" AT ";IHRMIN:
LPRINT
1210 IF QAV$="H" THEN GOTO 1360
1215 IF QAV$="L" THEN GOTO 1295
1220 ' AVERAGE WEEKLY DEPOSITION VELOCITIES AND OUTPUT THEM
1225 FOR M=1 TO 24
1230 IF NVDWK(M)=0 THEN GOTO 1285
1235 FOR L=1 TO NSPEC: AVVDWK(L,M)=AVVDWK(L,M)/NVDWK(M): NEXT L
1240 AVDPWK(M)=AVDPWK(M)/NVDWK(M)
1245 ITIME=(M*100)-70
1250 LPRINT USING FORMW1$;ITIME,NVDWK(M),AVVDWK(1,M)
1255 LPRINT USING FORMW2$;AVVDWK(2,M)
1260 LPRINT USING FORMW3$;AVVDWK(3,M)
1265 LPRINT USING FORMW4$;AVVDWK(4,M)
1270 LPRINT USING FORMW5$;AVVDWK(5,M)
1275 LPRINT USING FORMW6$;AVVDWK(6,M),AVDPWK(M)
1280 LPRINT
1285 NEXT M
1290 GOTO 1360
1295 FOR L=1 TO NSPEC: AVVDLAV(L)=0: NEXT L
1300 FOR M=1 TO 24
1305 FOR L=1 TO NSPEC: AVVDLAV(L)=AVVDLAV(L)+AVVDWK(L,M): NEXT L
1310 NVDLAV=NVDLAV+NVDWK(M): AVDPLAV=AVDPLAV+AVDPWK(M): NEXT M
1315 IF NVDLAV=0 THEN LPRINT "NO DATA AVAILABLE FOR CALCULATIONS": LPRINT:
GOTO 1360
1320 FOR L=1 TO NSPEC: AVVDLAV(L)=AVVDLAV(L)/NVDLAV: NEXT L
1325 AVDPLAV=AVDPLAV/NVDLAV
1330 LPRINT USING FORML1$;NVDLAV,AVVDLAV(1)
1335 LPRINT USING FORML2$;AVVDLAV(2)
1340 LPRINT USING FORML3$;AVVDLAV(3)
1345 LPRINT USING FORML4$;AVVDLAV(4)

```



```
1350 LPRINT USING FORML5$;AVVDLAV(5)
1355 LPRINT USING FORML6$;AVVDLAV(6),AVDPLAV
1360 BEEP
1365 PCPUMP=(HRSPUMP/HRSDATA)*100
1370 LPRINT: LPRINT USING "PUMP WAS FUNCTIONING PROPERLY ###.## PERCENT
(#### HOURS) OUT OF THE WEEK (#### HOURS TOTAL)";PCPUMP,HRSPUMP,HRSDATA
1375 END
```